

# Toric codes in topological quantum computation

Georgios Karaiskos

Supervisor: Emanuel Floratos, Professor Emeritus



Department of Nuclear and Particle Physics  
Faculty of Physics  
National and Kapodistrian University of Athens  
Greece  
March 6, 2021



## **Master's Thesis**

Submitted by Georgios Karaikos (Student ID: 2019209) to National  
Kapodistrian University of Athens,

Faculty of Physics, Department of Nuclear and Particle Physics,

in partial fulfilment of the requirements for the Master of Science with  
specialization in Physics.

### **Examination Committee:**

- Emmanuel Floratos, Professor Emeritus
- Alexandros Karanikas, Professor
- Fotios Diakonou, Associate Professor



## **Acknowledgment**

Foremost, I would like to express my sincere gratitude to my advisor Prof. Emanuel Floratos for the continuous support during the studying and writing of this thesis, for his patience, motivation and knowledge. I would also like to thank Prof. Fotios Diakonos and Prof. Alexandros Karanikas for taking the time to review this thesis and for participating in the examination committee. Last but not least, I would like to thank my friends and family for the spiritual support all this time.



## Abstract

For decades now, the realization of an operational quantum computer has captured the scientific community's interest. Such a device will be able to exploit the core concepts of quantum mechanics (superposition, entanglement) in order to solve specific problems, that would take an impractical amount of time for any conventional computer. The big obstacle we need to overcome for an idea like that to work is the sensitivity of quantum systems to what we call quantum noise. We begin our thesis by presenting the key ideas upon which the error correcting codes theory is structured. That is the theory responsible to deal with the fragile stability of quantum systems. The idea is to use a large number of physical quantum degrees of freedom (e.g. qubits) and restrict their possible states to a specific subspace of the original Hilbert space, hence, encoding a smaller number of logical quantum degrees of freedom.

We continue by analysing the most famous such code -the toric code- in a manner that gives birth to the concept of error correction at the physical level. What we, succinctly, do is introducing a Hamiltonian that involves only local interactions. The ground state of this Hamiltonian coincides with the subspace we talked about earlier. The degeneracy of that space, as well as its inaccessibility from local operations, makes it a prime candidate for safe quantum information storage. We then study the information process capabilities of this model.

Next comes a generalization of the toric code (called generalised Kitaev model) in which we use higher dimensional degrees of freedom to build our system. We analyse the new processes that emerge and see how these can aid our cause.

Finally we comment on the adequacy of our models to be used as topological quantum memories and briefly review the recent literature oriented towards the realisation of a more optimal model for the tasks of quantum information storage and process.





## Περίληψη

Εδώ και δεκαετίες η κατασκευή ενός λειτουργικού κβαντικού υπολογιστή έχει αιχμαλωτίσει το ενδιαφέρον της επιστημονικής κοινότητας. Μια τέτοια συσκευή θα μπορεί να εκμεταλλευτεί βασικές αρχές της κβαντικής μηχανικής (υπέρθωση, διεμπλοκή) ώστε να μπορεί να λύσει συγκεκριμένα προβλήματα, τα οποία οποιοςδήποτε κλασικός υπολογιστής θα χρειαζόταν τεράστιο (μη πρακτικό) χρόνο για να τα λύσει. Το μεγάλο πρόβλημα που πρέπει να ξεπεράσουμε για να δουλέψει αυτή η ιδέα είναι η ευαισθησία των κβαντικών συστημάτων σε αυτό που αποκαλούμε κβαντικό θόρυβο. Ξεκινάμε την εργασία μας παρουσιάζοντας τις βασικές ιδέες γύρω από την θεωρία των κωδικών διόρθωσης λαθών, της θεωρίας δηλαδή που έχει την ευθύνη να αντιμετωπίσει την εύθραυστη σταθερότητα των κβαντικών συστημάτων. Η ιδέα είναι να χρησιμοποιήσουμε έναν μεγάλο αριθμό φυσικών κβαντικών βαθμών ελευθερίας και να περιορίσουμε τις πιθανές καταστάσεις τους σε έναν συγκεκριμένο υπόχωρο του αρχικού χώρου Hilbert, άρα να κωδικοποιήσουμε έναν μικρότερο αριθμό λογικών, όπως τους αποκαλούμε, βαθμών ελευθερίας.

Συνεχίζουμε την ανάλυσή μας με τον πιο γνωστό τέτοιο κώδικα, τον toric code, με τρόπο ο οποίος γεννά την έννοια της διόρθωσης λαθών στο φυσικό επίπεδο. Συνοπτικά αυτό που κάνουμε είναι να εισάγουμε μια Χαμιλτονιανή που περιγράφει το σύστημά μας και έχει να κάνει αποκλειστικά με τοπικές αλληλεπιδράσεις. Δείχνεται ότι η θεμελιώδης κατάσταση αυτής της Χαμιλτονιανής συμπίπτει με τον υπόχωρο για τον οποίο μιλήσαμε νωρίτερα. Ο εκφυλισμός της θεμελιώδους κατάστασης καθώς και η μη δυνατή πρόσβαση σε αυτές τις καταστάσεις από τοπικές δράσεις, κάνουν τον χώρο αυτό κατάλληλο για την ασφαλή αποθήκευση της κβαντικής πληροφορίας. Ασχολούμαστε επίσης με την ικανότητα αυτού του μοντέλου για επεξεργασία της κβαντικής πληροφορίας.

Ακολουθεί η ενασχόλησή μας με το λεγόμενο γενικευμένο μοντέλο του Kitaev που χρησιμοποιεί ως φυσικούς βαθμούς ελευθερίας συστήματα περισσότερων διαστάσεων. Μελετάμε τις νέες διαδικασίες που αναδύονται σε αυτό το μοντέλο και βλέπουμε τι διαφορετικό έχει να μας προσφέρει.

Τέλος βλέπουμε το πόσο κατάλληλα είναι τα μοντέλα μας για να αποτελέσουν τοπολογικές κβαντικές μνήμες και κάνουμε ένα σύντομο σχολιασμό της σχετικής βιβλιογραφίας που προσπαθεί να απαντήσει στο σπουδαίο πρόβλημα της ασφαλούς αποθήκευσης και επεξεργασίας της κβαντικής πληροφορίας.



# Contents

<b>1</b>	<b>Introduction</b>	<b>4</b>
<b>2</b>	<b>Error correcting codes</b>	<b>5</b>
<b>3</b>	<b>Toric code</b>	<b>8</b>
3.1	Ground states . . . . .	13
3.2	Excitations . . . . .	15
3.2.1	Vertex excitations - charges . . . . .	15
3.2.2	Plaquette excitations - fluxes . . . . .	16
3.3	Fusion rules . . . . .	17
3.4	Anyonic statistics . . . . .	19
3.5	Error correction . . . . .	22
3.6	Toric code 2x2 example . . . . .	26
<b>4</b>	<b>Zd Kitaev model</b>	<b>31</b>
4.1	Anyon model . . . . .	35
4.2	Fusion process . . . . .	39
4.3	Anyon statistics . . . . .	40
4.4	Excitation Energy . . . . .	43
<b>5</b>	<b>Topological quantum memory</b>	<b>44</b>
5.1	Further work . . . . .	45
<b>6</b>	<b>Conclusion</b>	<b>47</b>



# 1 Introduction

The idea to merge quantum mechanics and information theory arose in the 1970s but garnered little attention until 1982, when physicist Richard Feynman gave a talk in which he reasoned that computing based on classical logic could not tractably process calculations describing quantum phenomena [1]. Computing based on quantum phenomena configured to simulate other quantum phenomena, however, would not be subject to the same bottlenecks. Though the interest on that field didn't really blossom until 1995 when Peter Shor came up with a quantum algorithm for integer factorization in polynomial-time [2]. The importance of this algorithm lies on the fact that nearly every cryptography method today relies on the intractability of the factoring problem to classical algorithms.

The difference between classical and quantum computers is the way they manipulate data in order to solve problems. While today's computers use bits as components of information, that is states that can be either 0 or 1, quantum computers aim to exploit two unique principles of quantum mechanics, superposition and entanglement, via their building blocks, the qubits (two level systems), in order to outpace their classical counterparts. In contrast to bits, qubits can be in a combination of the two states 0, 1 with varying probabilities (superposition), that is  $|\Psi\rangle = a|0\rangle + b|1\rangle$ . On the other hand entanglement or "spooky action at a distance" as Einstein famously described it refers to the ability to create pairs of qubits that exist in a single quantum state and changing the state of one instantaneously change the state of the other in a predictable way no matter the distance between them. These two principles lead us to a massive parallelism, meaning we can perform computations that are impossible for any classical computer (impossible here means that the computation takes an impractical amount of time). It is important to have in mind that those celebrated speed-ups that quantum computers have to offer are for specific problems. To find which those problems are, is a task on each own.

The biggest drawback in this world changing concept is how prone the quantum systems are to errors. Specifically the interaction of qubits with their environment in ways that cause their quantum behaviour to decay and ultimately disappear is called decoherence. Their quantum state is extremely fragile. The slightest vibration or change in temperature — disturbances known as noise — can cause them to tumble out of superposition before their job has been properly done. But even if we could isolate our system perfectly from the environment, in order to manipulate the qubits to do our bidding we are doomed to use imperfect gates (unitary operations) that lead

to errors. We deal with these problems via the theory of quantum error correcting codes [3, 4, 5]. But even so, the error threshold below which we can achieve fault tolerant quantum computation is really low.

What came next was Alexei Kitaev's game changing paper in 1997 [6] in which he proposes a topological quantum computation model that encodes information in the topologically degenerate ground states of a system and the computation is performed by braiding the quasiparticles of the model. Such a model is robust against local errors. The surface code, as it is called, is currently considered the most promising platform for realizing a scalable, fault tolerant quantum computer.

## 2 Error correcting codes

Let's take a look of the simplest classical error correcting code, the repetition code. In order to prevent a bit to change from 0 to 1 and the other way around (bit flip error) we make more copies of it, meaning:

$$0 \Rightarrow 000$$

$$1 \Rightarrow 111$$

If a single bit flip happens, say to the first bit then we have  $000 \Rightarrow 100$  and  $111 \Rightarrow 011$ . So by measuring all 3 bits and take the majority vote into consideration we can retract our information despite the error. Of course if we have two bits to flip then we going to get the wrong answer. But this is still better than doing nothing, considering that if  $p$  is the probability of a bit to flip then we managed to change the probability of making a mistake from  $p$  to  $\mathcal{O}(p^2)$ . The question is if we can do the same in order to protect some quantum information. This task has some serious difficulties:

- **Measurement.** In order to detect and correct the error in the classical repetition code we measured the bits. This process won't do here cause measuring a quantum state leads to its collapse meaning the superposition is destroyed and along with it our hopes of quantum advantage.
- **No cloning theorem.** There is no quantum operation that will take an arbitrary state  $|\Psi\rangle$  to  $|\Psi\rangle \otimes |\Psi\rangle$  for all states  $|\Psi\rangle$ . This fact is a simple consequence of the linearity of quantum mechanics.
- **Multiple errors.** Except from the bit flip errors, a quantum state is also frail to phase flip errors.

- Continuous notations and decoherence. As we know quantum information is continuous and as such it may lapse into a smaller error than a whole phase flip. There is also the case of mixtures of different kind of errors.

Fortunately for us Peter Shor showed we can cope with all these difficulties relatively easy [3]. We are not going to follow the analysis of quantum error correcting codes step by step but we are going to highlight the key points that are gonna be of use (a clear review on the matter is given in [4]). It turns out that if a quantum error correcting code (QECC) corrects errors A and B, it also corrects any linear combination of them,  $aA + bB$ . So if we can correct single qubit errors of X (bit flip), Z (phase flip), Y (bit and phase flip), I (no errors) we can correct every single qubit error cause as we know any  $2 \times 2$  matrix can be written as  $aI + bX + cY + dZ$ , where X, Y, Z are the Pauli matrices in the base  $|0\rangle, |1\rangle$ . As a generalisation any QECC that corrects t-qubit errors X, Y, Z, I on t-qubits also corrects all t-qubit errors, as any  $2^t \times 2^t$  matrix can be written as a tensor product of Pauli matrices.

With these in mind we continue on presenting a formalism that helps deal with QECC and makes finding and correcting errors a lot easier. As we saw the Pauli matrices play a crucial role to the whole procedure. Let us define the Pauli group  $P_n$  on n qubits to be generated by X, Y, Z, I on individual qubits. Then  $P_n$  consists of all tensor products of up to n operators X, Y, Z, I with overall phase  $\pm 1, \pm i$ . It emerges from Pauli matrices commutation relationships that all elements of Pauli group either commute or anticommute. Also they all square to  $\pm 1$  with the minus coming from the overall phase i.

We now define the stabilizer group S as a group that contains all operators M in the Pauli group for which  $M|\Psi\rangle = |\Psi\rangle$  for all  $|\Psi\rangle$  in the code (the space we want to protect). We note that the stabilizer group is Abelian meaning that all its elements commutes with each other:

$$\begin{cases} M|\Psi\rangle = |\Psi\rangle \\ N|\Psi\rangle = |\Psi\rangle \end{cases} \Rightarrow (MN - NM)|\Psi\rangle = MN|\Psi\rangle - NM|\Psi\rangle = 0$$

So we got  $MN = NM \quad \forall M, N \in S$ .

A much easier and useful procedure is to come up with a stabilizer group and from that deduce a code space as:

$$T(S) = \{|\Psi\rangle : M|\Psi\rangle = |\Psi\rangle \quad \forall M \in S\} \quad (1)$$

If we do this and we have a stabilizer code that has  $r$  generators and  $n$  physical qubits then we will have  $k = n - r$  logical qubits. We can think of that as starting in a Hilbert space of dimension  $2^n$ . Every generator demands eigenvectors of  $+1$  thus cutting the Hilbert space in half, that is dimension  $2^{n-1}$ . If we keep on going we end up with a Hilbert space of dimension  $2^{n-r}$  giving us  $k$  logical qubits. We need to take extra caution for the fact that every new generator must also cut the remaining Hilbert space in half, but it can be proved that this is the case for the Pauli group.

We are now ready to see how stabilizer elements detect errors. Suppose  $M \in S$  and Pauli error  $E$  anticommute with each other. Then:

$$M(E|\Psi\rangle) = -EM|\Psi\rangle = -E|\Psi\rangle \quad (2)$$

As it is clear  $E|\Psi\rangle$  is an eigenvector of  $M$  with eigenvalue  $-1$ . Thus error  $E$  kicks our state out of the code space, a process we can easily detect. But what happens when  $E$  commutes with all  $M \in S$ ? Then obviously all  $M$ s have eigenvalues  $+1$  for the state  $E|\Psi\rangle$ . As we are about to see this can mean one of two things. Either we have an undetectable error or we have no error at all.

We define:

$$N(S) = \{N \in P_n : MN = NM \quad \forall M \in S\} \quad (3)$$

So if  $E \in N(S)$ , our stabilizers won't be able to detect the error. One special case that leads to commutation between our error and all the stabilizers is  $E \in S$ . But if we think of that we see that this does not qualify as an error at all, cause  $S$ 's define property is that it leaves the code unchanged, that is act on it like the identity. We conclude that our code detects any error that is not in the  $N(S) \setminus S$ .

One very important concept is that of the distance of the code. By this we mean the weight (the number of qubits on which we act non-trivially) of the smallest Pauli operator  $N$  in  $N(S) \setminus S$  or to phrase it simpler the size of the smallest undetectable error. The error syndrome is the list of eigenvalues of the generators of  $S$ . Two errors say  $E, F$  have the same error syndrome iff  $E^\dagger F \in N(S)$  that is  $E^\dagger F$  commutes with everything in the stabilizer. We notice that if  $E^\dagger F \in S$  then  $E, F$  cannot be distinguished, as both (different) errors do the same thing to our code. So correcting one corrects the other and vice versa. This quality will be of tremendous benefit in the error correction procedure. To sum up the condition for our stabilizer code to correct errors is:

$$E^\dagger F \notin N(S) \setminus S \quad \text{for all possible pairs of errors } (E, F)$$



There is also a straightforward generalization of the class of stabilizer codes to  $d$ -dimensional systems as described in [5]. From now on we are going to attend to a special case of stabilizer quantum codes associated with lattices on the torus. These topological, as they called, codes stores information in topologically protected space of the system and thus embed it with local error robustness. Moreover we are not going to use the usual scheme of error correction, rather we are going to implement error correction at the physical level as presented in Kitaev's original paper [6]. The analysis that follows shows the geometrical interpretation of the above concepts when they are applied to topological systems.

### 3 Toric code

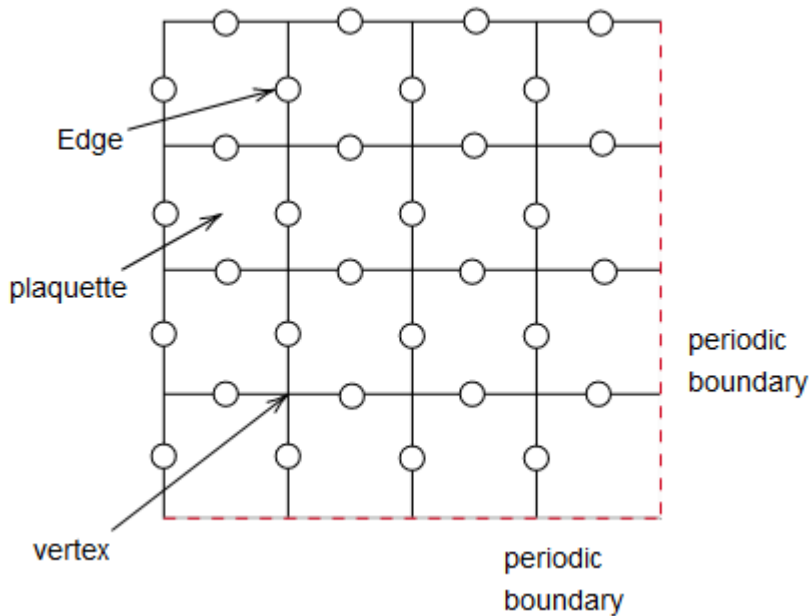


Figure 1: The toric code is defined in terms of a  $k \times k$  lattice (here  $k = 4$ ) with periodic boundary conditions. Edges, plaquettes and vertices are all important concepts. Edges have circles embedded on them, which will represent qubits.

Consider a  $k \times k$  square lattice with periodic boundary conditions on both space directions (thus forming a torus)(Figure 1). The lattice consists

of edges ( $E$ ), vertices (points where edges meet)( $S$ ) and plaquettes/faces (individual tiles enclosed by a set of edges - here squares) ( $P$ ). Let us attach a spin, or a qubit (two level quantum system), to each edge of the lattice. (Thus there are  $n = 2k^2$  qubits).

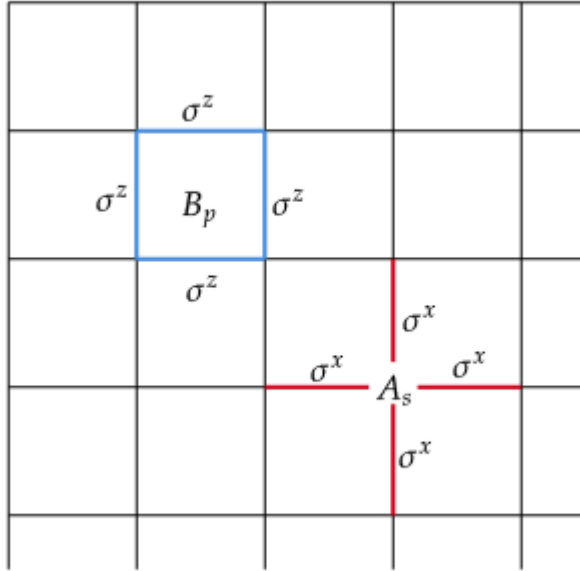


Figure 2: Toric code's stabilizer operators.

For each vertex  $s$  and each face  $p$  we define the following operators:

$$A_s = \prod_{j \in \text{star}(s)} \sigma_j^x, \quad B_p = \prod_{j \in \text{boundary}(p)} \sigma_j^z \quad (4)$$

where  $A_s$  acts on the star qubits ( i.e the qubits lying on the edges neighbouring the  $s$  vertex ) by the Pauli operator  $\sigma^x$ , and to all other qubits of the lattice with the identical operator, namely:

$$\sigma_j^x = \underbrace{I \otimes \dots \otimes I}_{(j-1)\text{times}} \otimes \sigma^x \otimes \underbrace{I \otimes \dots \otimes I}_{(2k^2-j)\text{times}} \quad (5)$$

and  $B_p$  acts on the face qubits (i.e the qubits lying on the edges that enclose the  $p$  face) by the Pauli operator  $\sigma^z$ , and to all other qubits with the identical

operator, namely:

$$\sigma_j^z = \underbrace{I \otimes \cdots \otimes I}_{(j-1)\text{times}} \otimes \sigma^z \otimes \underbrace{I \otimes \cdots \otimes I}_{(2k^2-j)\text{times}} \quad (6)$$

See Figure 2. Thus both of these operators are of weight 4. In order to study these operators it is useful to recall some properties of the Pauli matrices:

$$\sigma^x = \begin{pmatrix} 0 & 1 \\ 1 & 0 \end{pmatrix}, \quad \sigma^y = \begin{pmatrix} 0 & -i \\ i & 0 \end{pmatrix}, \quad \sigma^z = \begin{pmatrix} 1 & 0 \\ 0 & -1 \end{pmatrix} \quad (7)$$

We work in the basis that respects  $\sigma^z$ , thus spanned by the vectors:

$$|0\rangle = \begin{pmatrix} 1 \\ 0 \end{pmatrix}, \quad |1\rangle = \begin{pmatrix} 0 \\ 1 \end{pmatrix} \quad (8)$$

giving the following action of the  $\sigma^z$  and  $\sigma^x$  operators:

$$\sigma^z |0\rangle = |0\rangle, \quad \sigma^z |1\rangle = -|1\rangle \quad (9)$$

$$\sigma^x |0\rangle = |1\rangle, \quad \sigma^x |1\rangle = |0\rangle \quad (10)$$

Starting with their commutation relationships we have:

$$\sigma_j^a \sigma_k^b = \begin{cases} -\sigma_k^b \sigma_j^a & a \neq b, \quad j = k \\ \sigma_k^b \sigma_j^a & \text{otherwise} \end{cases}$$

These expressions fix the commutation relations of the operators  $A_s$  and  $B_p$ . It is clear that all  $A_s$  commute with each other just as all  $B_p$  commute with each other, meaning  $[A_s, A_{s'}] = 0 \quad \forall s, s' \in S$  and  $[B_p, B_{p'}] = 0 \quad \forall p, p' \in P$ . The commutation relation between  $A_s$  and  $B_p$  is slightly less trivial. We start with the observation that a face and a vertex can either share two edges or none. With no edges in common the commutation is profound whereas with two edges in common the anticommutation relationship between  $\sigma^x$  and  $\sigma^z$  gives two minus signs which co-cancel, so again the operators in question commutes to give an overall:

$$[A_s, B_p] = 0 \quad \forall s, p$$

Next we make use of the fact that Pauli operators square to unity:

$$(\sigma^x)^2 = (\sigma^y)^2 = (\sigma^z)^2 = 1$$

From the above it is straightforward to see that this is also the case for our check operators, meaning:

$$A_s^2 = B_p^2 = 1 \Rightarrow A_s, B_p = \pm 1$$

That is, if we apply the vertex (plaquette) operator twice on a given state it will remain unchanged. It is of interest to see what happens if we apply vertex (plaquettes) operators on adjacent vertices (plaquettes). Given that any two adjacent vertices (plaquettes) share a common edge, we end up acting on that edge with the identity operator. We can convince ourselves that this process leads to the creation of closed loops (they materialize by colouring the edges, that our system operators have acted upon non trivially), either on the dual lattice<sup>1</sup> (if it's vertex operators we work with) or on the primal lattice (for plaquette operators), that enclose the vertices/plaquettes in question (Figure 3).

If we now extend this analysis for the case when we apply vertex (plaquette) operators to the entire lattice, the result will leave all edges without any change, giving the following overall constrains:

$$\prod_s A_s = \prod_p B_p = I \tag{11}$$

Let  $\mathcal{N}$  be the Hilbert space of all  $n = 2k^2$  qubits, thus a Hilbert space of dimension  $2^{2k^2}$ . Define a protected subspace  $\mathcal{L} \subseteq \mathcal{N}$  as follows:

$$\mathcal{L} = \{|\Psi\rangle \in \mathcal{N} : A_s |\Psi\rangle = |\Psi\rangle, B_p |\Psi\rangle = |\Psi\rangle \forall s, p\} \tag{12}$$

This equation serves as the definition of the toric code with  $A_s$  and  $B_p$  being the stabilizer operators (generators of the stabilizer group). The dimensionality of this subspace is given by  $\dim \mathcal{L} = 2^{n-m}$  where  $n$  is the number of physical qubits and  $m$  the independent stabilizer operators. Thus for a lattice wrapped around a torus this protected subspace is 4 dimensional, and so can be used to store two qubits of quantum information. Now let's consider operators of the form:

$$X(c') = \prod_{j \in c'} \sigma_j^x, \quad Z(c) = \prod_{j \in c} \sigma_j^z \tag{13}$$

where  $c'$  is a path forming a loop in the dual lattice and  $c$  a path forming a loop in the primal lattice. It is straightforward from the above analysis

---

<sup>1</sup>We construct the dual lattice by  $\pi/2$  rotation of the primal lattice, so the vertices become plaquettes and the plaquettes become vertices.

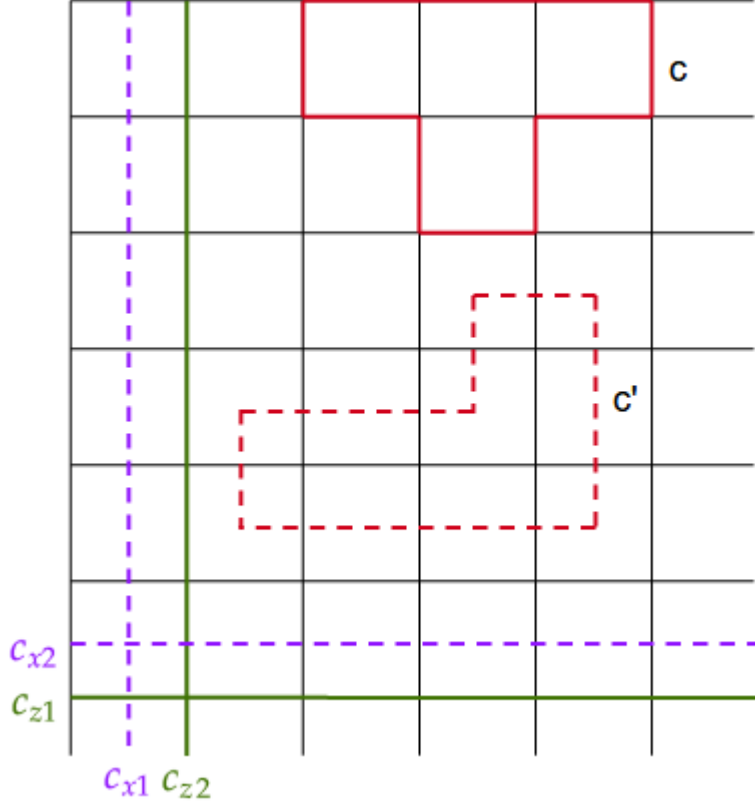


Figure 3: Loops on the lattice and the dual lattice.

that these operators can be constructed by the product of stabilizer operators. We call these loops  $(c, c')$ , contractible loops, as they are homotopy equivalent to a point, meaning we can deform them continuously to a point. We can also construct non-contractible loops, that is loops that wind the torus in its horizontal and vertical direction and thus cannot be written as products of stabilizer operators and neither can they be deformed to a point (Figure 3). These are loops of different topology. We label these paths as  $c_{x1}, c_{x2}, c_{z1}, c_{z2}$  and the operators related to them as  $\tilde{X}_1, \tilde{X}_2, \tilde{Z}_1, \tilde{Z}_2$ . The connection between these kind of loops (and so the topology of our surface) and the degeneracy of the toric code space will be apparent later on. To

make a bridge with the previous section we note that the operators (13) belong to the stabilizer group hence do not identify as errors at all while the ones attached to the non contractible loops are the ones that pose a grave danger to our model, being undetected and all. The operators (13) can as well be defined to act on domains corresponding to open paths, with a significant impact to our model, as we are going to see. These are the detectable errors of our model, available for correction. So we have constructed a QECC who can protect our code via the usual procedure of error detection (through error syndrome measurement) and error correction. Before we construct the code space and work these procedures explicitly we are going to see another interpretation of that code that affiliates it with the physical level.

For that purpose let us define a Hamiltonian as the sum of plaquette and vertex operators over all plaquettes and vertices of the lattice:

$$H = - \sum_s A_s - \sum_p B_p \quad (14)$$

Since all terms in this Hamiltonian commutes, (14) can be easily diagonalized in the basis of the eigenstates of the  $A_s$  and  $B_p$  operators, that is it can be exactly solved. In the following sections we discuss the ground states as well as the excited states of our Hamiltonian and see how the error resistance in the physical level is achieved.

### 3.1 Ground states

To find the ground state  $|\Psi\rangle$  of H we need to find the condition that minimize the energy. Given the form of the Hamiltonian and the fact that  $A_s$  and  $B_p$  have eigenvalues  $\pm 1$ , the condition of minimum energy is equivalent to that of:

$$A_s |\Psi\rangle = |\Psi\rangle, \quad B_p |\Psi\rangle = |\Psi\rangle \quad \forall s, p$$

creating the following space of ground states:

$$L = \{|\Psi\rangle : A_s |\Psi\rangle = |\Psi\rangle, B_p |\Psi\rangle = |\Psi\rangle \quad \forall s, p\} \quad (15)$$

We see that the ground state space coincides with the protected subspace of the toric code. In the gap between the ground states and the excited ones partially lies the physical protection of our code. This will be elaborated after a few sections. The energy of the ground state is given by  $E_{min} = -(P + S) = -2k^2$ , where P is the number of plaquettes ( $k^2$ ) and S the

number of vertices ( $k^2$ ) of our  $k \times k$  lattice. We argue that the ground state is given by (up to a normalization):

$$|\Psi\rangle = \prod_s (I + A_s) |0\rangle^{\otimes n} \quad (16)$$

This is easily proved by checking that our constraints hold:

$$\begin{aligned} B_p \prod_s (I + A_s) |0\rangle^{\otimes n} &= \prod_s (I + A_s) B_p |0\rangle^{\otimes n} \\ &= \prod_s (I + A_s) |0\rangle^{\otimes n} \end{aligned} \quad (17)$$

where in the first line we used  $[B_p, A_s] = 0 \forall s, p$ , and for the second line that  $B_p |0\rangle^{\otimes n} = |0\rangle^{\otimes n} \forall p$ .

As for the second constraint we have:

$$A_s \prod_s (I + A_s) |0\rangle^{\otimes n} = \prod_s (I + A_s) |0\rangle^{\otimes n} \quad (18)$$

where we used the fact that  $(A_s)^2 = I$ .

We see that the ground state is the equal superposition of all possible products of elementary loops  $A_s$ . Application of any contractible loop operator on the ground state gives back the same state with its components rearranged. But what will we get if we apply a non-contractible loop? As will be shown in the next section we still are on a ground state of our system (after all the operators responsible for these loops commute with all our stabilizers), but on a different one. Thus we conclude that there is a degeneracy on the ground state, one that goes hand in hand with the non-contractible loops (of  $\sigma^x$  operators) of our model, or more accurately with the parity of the winding number around the torus in each space direction (each handle of the torus). More specifically for an odd winding number around the torus we get a new ground state, thus we get an overall of 4 ground states. One with even winding number in both vertical and horizontal directions, one with odd winding number in the horizontal direction and an even number in the vertical direction, one with even winding number in the horizontal direction and odd in the vertical and finally one with odd winding numbers in both directions. To sum up we have:

$$|\Psi^{(0)}\rangle, |\Psi^{(1)}\rangle = \tilde{X}_2 |\Psi^{(0)}\rangle, |\Psi^{(2)}\rangle = \tilde{X}_1 |\Psi^{(0)}\rangle, |\Psi^{(3)}\rangle = \tilde{X}_1 \tilde{X}_2 |\Psi^{(0)}\rangle$$

The toric code Hamiltonian can be seen as a lattice gauge theory [7]. In this framework the degrees of freedom living on the edges of the lattice correspond to  $\mathbb{Z}_2$  (note that this is the symmetry of our model since  $\sigma^\dagger = \sigma^{-1} = \sigma^2$ ) valued gauge degrees of freedom, the vertex operator corresponds to a gauge transformation, and since it commutes with the plaquette operator implies an overall gauge invariance. It is from this equivalence to a gauge theory that the excitations of the toric code that come from violating one of the conditions in Eq.(15) are commonly known as charges and fluxes as we will see in the next section.

### 3.2 Excitations

We have seen in the previous section that a ground state  $|\Psi\rangle$  is defined by the following constraints:

$$A_s |\Psi\rangle = |\Psi\rangle \quad (19)$$

$$B_p |\Psi\rangle = |\Psi\rangle \quad (20)$$

An elementary excitation or a 1-particle excitation (in the quasi-particle picture) is defined by the violation of exactly one of these constraints. Having in mind that the  $A_s$ 's and  $B_p$ 's are not independent operators (eq. 11), it is impossible to have exactly one  $A_s$  or one  $B_p$  violated, which means single particle excitations do not exist (its a direct consequence of the fact that every edge on the lattice is shared between two vertices and two plaquettes). Let's consider the two-particle excitations.

#### 3.2.1 Vertex excitations - charges

Suppose we have one of our vacuum states, say  $|\Psi\rangle$ , and act on it with an operator  $\sigma_i^z$ , that is we act with the operator  $\sigma^z$  (phase flip) on the  $i$ -th edge (qubit) of the lattice. Then we get the following state:

$$|\Psi_i^z\rangle = \sigma_i^z |\Psi\rangle \quad (21)$$

which is short for:

$$|\Psi_i^z\rangle = \underbrace{I \otimes \dots \otimes I}_{(i-1)\text{times}} \otimes \sigma_i^z \otimes \underbrace{I \otimes \dots \otimes I}_{(2k^2-i)\text{times}} |\Psi\rangle$$

This new state is no longer a ground state. The  $\sigma_i^z$  may clearly commute (and thus preserve the constraints) with all the  $B_p$  operators and with the majority of the  $A_s$  operators but there are exactly two vertex operators,



the ones adjacent to the  $i$ -th edge that anticommute with it leading to the following constrains violation:

$$A_{s_1, s_2} |\Psi_i^z\rangle = A_{s_1, s_2} \sigma_i^z |\Psi\rangle = -\sigma_i^z A_{s_1, s_2} |\Psi\rangle = -\sigma_i^z |\Psi\rangle = -|\Psi_i^z\rangle \quad (22)$$

In this sense we say that  $\sigma_i^z$  creates two excitations located at vertices  $s_1, s_2$ . We interpret these excitations as anyonic (due to their statistics as we will soon see) quasiparticles.

Let's see what happens if we act on the ground state with various  $\sigma^z$  operators along an open path  $t$  (Figure 4) i.e with the so called string operator:

$$Z(t) = \prod_{j \in t} \sigma_j^z \quad (23)$$

It is obvious that the only violation in constrains happens at the end points of this path, whereas the intermediate  $A_s$ 's due to the commutation of  $(\sigma^x \otimes \sigma^x)(\sigma^z \otimes \sigma^z)$  gives no violation. From these we deduce a way to move vertex anyons through our lattice. Note that if this path equals a closed loop then we have no excitations (remember a contractible loop acts like the identity on our code space). It is like creating a pair of anyons and then bringing them together via another route. That causes their annihilation and thus the return to the anyonic vacuum (ground state). More on that in the fusion section. We will call the vertex anyons (a result of phase flip errors) charges and denote them with  $e$ .

The energy of a state with a pair of  $e$  charges is given by:

$$E = -(P + S - 4) \quad (24)$$

which explains the term excitation and also justifies our claim of robustness in errors at the physical level, due to the fact that excited states are energetically penalized by the energy gap between the ground states and the excited ones. It is obvious that this energy gap has to do with the number of charges (that is the number of  $A_s$  constrains violated) and not with the path that created them.

### 3.2.2 Plaquette excitations - fluxes

An analogues scheme can be plotted in order to explore the  $B_p$ 's constraints violation. Consider the string operator:

$$X(t) = \prod_{j \in t'} \sigma_j^x \quad (25)$$

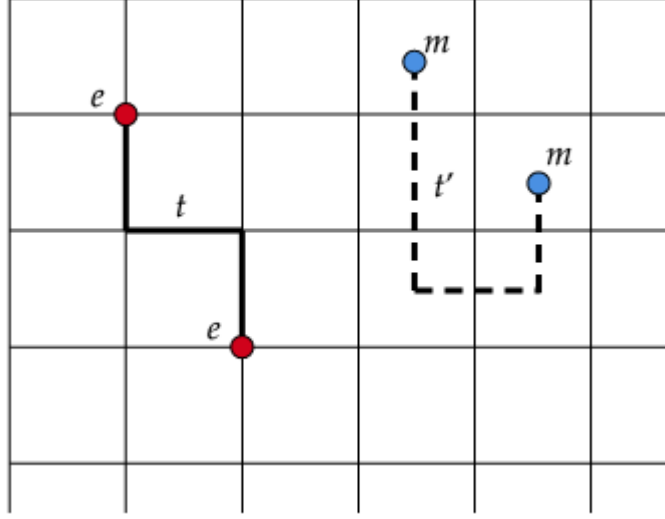


Figure 4: String operators and particle creation.

where  $t'$  is a path on the dual lattice, connecting plaquettes (Figure 4). Again on the endpoints of this path we locate two violations considering the  $B_p$ 's stabilizer operators on place. We call the plaquette violations (a result of bit flip errors), fluxes and denote them with  $m$ . As with the charge excitations, the energy of our new state is  $E = -(P + V - 4)$  and does not depend on the path.

### 3.3 Fusion rules

The fusion of the particles of our model is one of the key procedures for quantum computation. But what do we mean by fusion of our particles? Suppose we got two vertex anyons that do not consist a pair. That means they are not connected with each other by a string (see Figure 5). So our initial state is:

$$|\Psi_{in}\rangle = Z(\gamma_1)Z(\gamma_2)|\Psi\rangle \quad (26)$$

Now let's bring those two together by moving either one of them through the path  $\gamma_3$ . That move has as a result the annihilation of the two  $e$  particles, that is the commutation of our newly acquired string operator with the previously engaged vertex operators ( $s, s'$ ). Thus we say when we fuse these

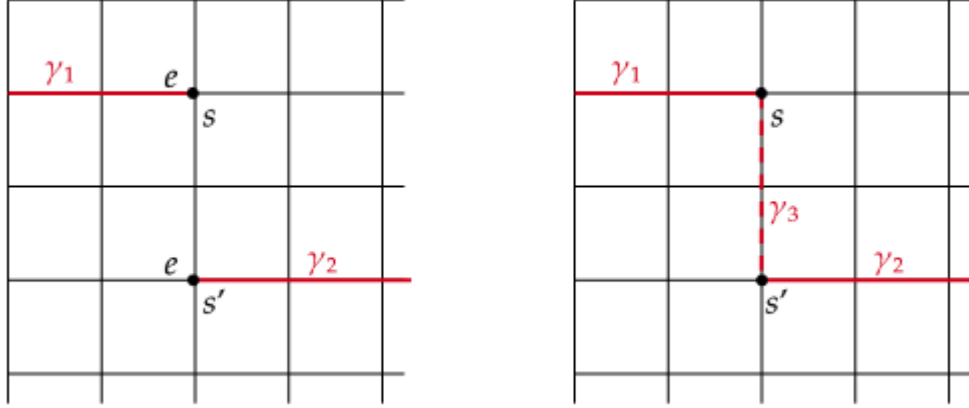


Figure 5: The fusion process of two vertex anyons that leads to their mutual annihilation

two together they cancel each other out, leading to the following fusion rule:

$$e \times e = 1$$

where 1 signals the absence of an excitation.

In an analogous manner we come up with the fusion rule for the plaquette anyons:

$$m \times m = 1$$

From these we deduce that both vertex and plaquette particles have themselves as antiparticles (which should have been clear the moment we created a pair of each from the anyonic vacuum). We can see clearer now what we mean by  $\mathbb{Z}_2$  symmetry of our model. The anyonic charge is preserved modulo 2.

Lastly let's consider the case in which we simultaneously act on an edge with both a bit ( $\sigma^x$ ) and a phase ( $\sigma^z$ ) flip. That leads, as we see in Figure 6, to the creation of an e-type particle to a vertex and an m-type anyon to an adjacent plaquette. We can interpret these excitations as one and call it dyon. This interpretation gives birth to yet another fusion rule:

$$e \times m = \epsilon$$

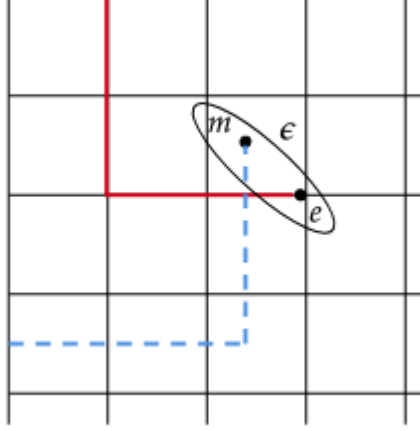


Figure 6: The interpretation of an  $e$  and an  $m$  excitation as one particle named dyon

So now we are ready for a full categorization of the anyons of our model:

$$1, e, m, \epsilon \quad (27)$$

and their fusion rules:

$$1 \times 1 = 1, \quad 1 \times e = e \times 1 = e, \quad 1 \times m = m \times 1 = m, \quad e \times m = m \times e = \epsilon, \\ e \times \epsilon = \epsilon \times e = m, \quad m \times \epsilon = \epsilon \times m = e, \quad m \times m = e \times e = \epsilon \times \epsilon = 1$$

The deterministic nature of these fusion rules tells us that we are talking about Abelian anyons.

### 3.4 Anyonic statistics

We now study the statistical behaviour of the elementary excitations of the model, namely the charge  $e$ , the flux  $m$  and the dyon  $\epsilon$ . Consider two  $e$  anyons as shown in Figure 7. Our system is on the state  $|\Psi_{in}\rangle = Z(\gamma_1)Z(\gamma_2)|\Psi\rangle$ . We can exchange their position by applying  $\sigma^z$  rotations. The process goes as follows:

$$|\Psi_{fin}\rangle = Z(c_1)Z(c_2)|\Psi_{in}\rangle = |\Psi_{in}\rangle \quad (28)$$

where the last equation comes from the fact that we have created a contractible loop which does not contain a flux, thus acts trivially on our state.

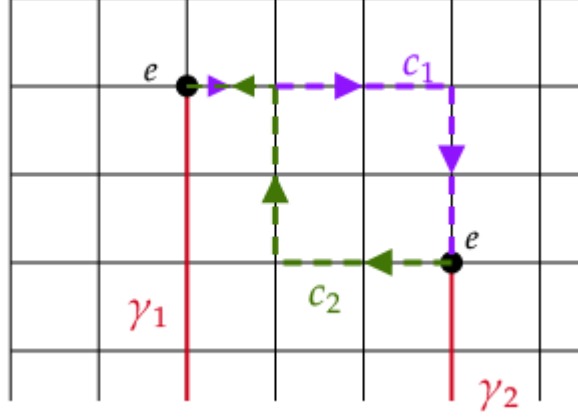


Figure 7: Exchange of two identical e anyons.

The excited states inherit this property, from the ground ones, by being the equal superposition of all possible strings that connect the two anyons. Hence, the final state of the system equals the initial one, thereby signalling the bosonic mutual statistics of e anyons. With exactly analogous arguments we conclude that m anyons behave like bosons too, when it comes to their self-statistics.

As the e and the m anyons are distinguishable, we cannot directly exchange them, but we can braid them. Braiding corresponds to two exchanges, or equivalently a rotation of one anyon around the other, from where we can attribute their exchange statistics as the square root of the resulting evolution. Following Figure 8 we start from an anyonic vacuum state and create a pair of e-type anyons and a pair of m-type anyons via the usual procedure:

$$|\Psi_{in}\rangle = \sigma_1^z \sigma_2^z \sigma_3^x \sigma_4^x |\Psi\rangle \quad (29)$$

Next we circle an m anyon with an e anyon using the path t:

$$\begin{aligned} |\Psi_{fin}\rangle &= Z(t) |\Psi_{in}\rangle = Z(t) \sigma_1^z \sigma_2^z \sigma_3^x \sigma_4^x |\Psi\rangle \\ &= -\sigma_1^z \sigma_2^z \sigma_3^x \sigma_4^x Z(t) |\Psi\rangle \\ &= -\sigma_1^z \sigma_2^z \sigma_3^x \sigma_4^x |\Psi\rangle \\ &= -|\Psi_{in}\rangle \end{aligned} \quad (30)$$

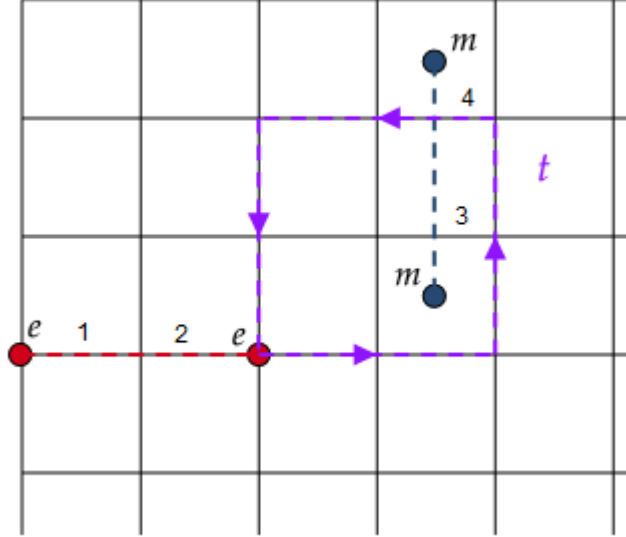


Figure 8: Braiding of a charge anyon  $e$  around a flux anyon  $m$ .

where in the second line we used the anticommutation relation between  $\sigma_4^z$  of the path that moves  $e$  and  $\sigma_4^x$  of the creator of the  $m$ -pair anyons and on the third line the fact that  $t$  is a contractible loop, hence does not affect the ground state. The topological phase factor of  $-1$  reveals a non-trivial statistics between  $e$  and  $m$  anyons that does not suit neither bosons nor fermions, signaling the anyonic character between different types of particles of the toric code. We call it topological because it depends not on the exact route of the braiding process but from the winding number. It can also be interpreted as a Aharonov-Bohm effect (remember the charge, flux interpretation).

Last we check the exchange statistics for the dyon. Having in mind the structure of the dyon it is easy to see that this process equals a rotation of the particle by  $2\pi$  around itself. But this we have already seen. It gives a topological phase of  $-1$  so that dyons are fermions, with respect to themselves.

The anyonic mutual statistics of the quasiparticles demonstrate the logical operations performed by non contractible loops. How can i create a non-contractible loop operator using the anyon picture? Consider the cre-

ation of a pair of  $e$  anyons followed by the transport of one around a handle of the torus (i.e a non trivial loop), such as the one shown on the torus in blue on Figure 9, before the pair are re-annihilated. The state is returned to the code space, but the loop implements a logical operation on one of the stored qubits. It is the  $\tilde{Z}_2$  operator we talked about earlier. If  $m$  anyons are similarly moved through the red loop, a logical operation will also result ( $\tilde{X}_2$ ). The phase of  $-1$  resulting when braiding the anyons shows that these operations anticommute. They may therefore be interpreted as logical  $Z$  and  $X$  Pauli operators on one of the stored qubits. The corresponding logical Pauli's on the other qubit correspond to an  $m$  anyon following the blue loop and an  $e$  anyon following the red. No braiding occurs when  $e$  and  $m$  pass through parallel paths, the phase of  $-1$  therefore does not arise and the corresponding logical operations commute. This is as should be expected since these form operations acting on different qubits. Thus in order to mess with our information we need global operations. Local errors cannot access our encoded qubits, giving us the protection we so desperately seek.

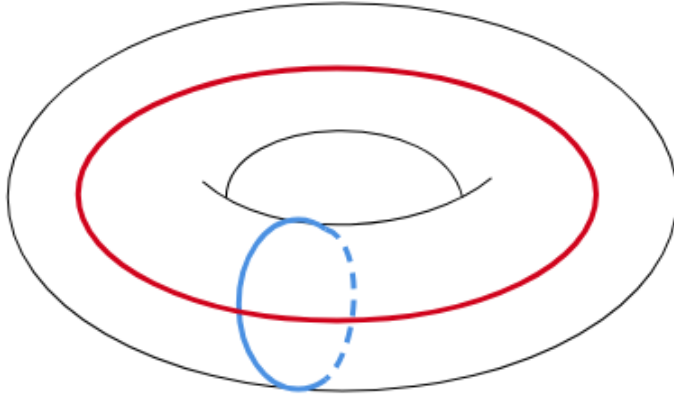


Figure 9: Torus.

### 3.5 Error correction

Although our model have an intrinsic topological protection from errors, assuming that the environment can only probe the system locally by applying small static perturbations to the Hamiltonian, given a finite error rate and long enough time, independent local errors in the theory will eventually

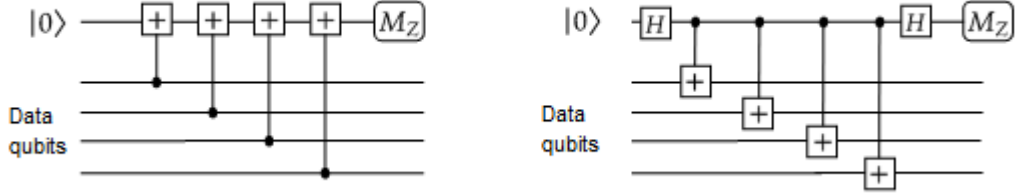


Figure 10: Check operators measurements. The left circuit is for the  $Z^{\otimes 4}$  measurement while the right circuit is for the  $X^{\otimes 4}$  measurement.

accumulate to form a global operation, and result in a logical error. Thus we still need an error correcting code procedure. By measuring the stabilizers we can detect any error that occurred to our code (except the ones that lead to logical operations). This error syndrome measurement can be achieved by the circuits in Figure 10. Interpreting the  $-1$  results as anyonic particles, and as a matter of fact particles that are their own antiparticles, means we only have to bring them together in order to annihilate them and thus correct the error. The fact that a contractible loop does not affect our state, which as we already mentioned is a reflection to the fact that we can not distinguish two errors for which  $E^\dagger F \in N(S)$  (see ECC section), makes our life a lot easier though we need not to concern ourselves with the specific path that created the pair errors. We only need to know their exact locations and then any route connecting them will do the job. In order to avoid committing a logical mistake, thus compromise our information, the rule of minimum correcting path is chosen. Meaning we choose to connect the two anyons via the shortest path. It is obvious that our scheme will fail for errors of length bigger than  $\frac{k-1}{2}$ .

Let's take a look at the two cases in Figure 11. For the upper one we have the error:

$$E_1 = \sigma_7^x \otimes \sigma_{11}^x \otimes \sigma_{15}^x$$

leading to the state:

$$|\Psi'\rangle = E_1 |\Psi\rangle \tag{31}$$



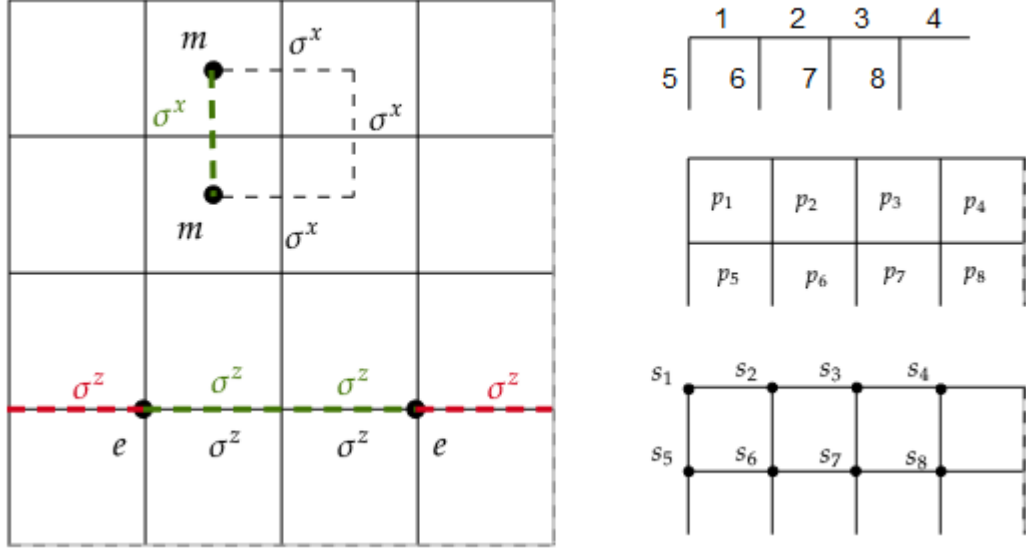


Figure 11: On the upper half of this diagram we see that even if we do not find the correct route that led to the error we can still correct it without a problem. On the bottom half we see that when an error is of length  $k/2$  there is a good chance of choose the wrong route to correct (red) instead of the right (green) and by that we imply unwillingly a logical operator to the code. Next to the diagram its a sketch about the enumeration of the edges, the plaquettes and the vertices.

It is obvious that for  $p_2, p_6$  we have:

$$\begin{aligned}
B_{p_2} E_1 |\Psi\rangle &= (\sigma_2^z \otimes \sigma_6^z \otimes \sigma_7^z \otimes \sigma_{10}^z) (\sigma_7^x \otimes \sigma_{11}^x \otimes \sigma_{15}^x) |\Psi\rangle \\
&= -(\sigma_7^x \otimes \sigma_{11}^x \otimes \sigma_{15}^x) (\sigma_2^z \otimes \sigma_6^z \otimes \sigma_7^z \otimes \sigma_{10}^z) |\Psi\rangle \\
&= -E_1 B_{p_1} |\Psi\rangle = -E_1 |\Psi\rangle \\
B_{p_6} E_1 |\Psi\rangle &= (\sigma_{10}^z \otimes \sigma_{14}^z \otimes \sigma_{15}^z \otimes \sigma_{18}^z) (\sigma_7^x \otimes \sigma_{11}^x \otimes \sigma_{15}^x) |\Psi\rangle \\
&= -(\sigma_7^x \otimes \sigma_{11}^x \otimes \sigma_{15}^x) (\sigma_{10}^z \otimes \sigma_{14}^z \otimes \sigma_{15}^z \otimes \sigma_{18}^z) |\Psi\rangle \\
&= -E_1 B_{p_6} |\Psi\rangle = -E_1 |\Psi\rangle
\end{aligned} \tag{32}$$

Thus in each of these plaquettes we have an m-type anyon. Let's see what will happen if we apply the following correction:

$$C_1 = \sigma_{10}^x \tag{33}$$

We notice that the stabilizer operators of the plaquettes in question  $(p_2, p_6)$  commute with the operator  $C_1 E_1 = \sigma_7^x \otimes \sigma_{10}^x \otimes \sigma_{11}^x \otimes \sigma_{15}^x$  :

$$\begin{aligned} B_{p_2}(C_1 E_1) &= (\sigma_2^z \otimes \sigma_6^z \otimes \sigma_7^z \otimes \sigma_{10}^z) (\sigma_7^x \otimes \sigma_{10}^x \otimes \sigma_{11}^x \otimes \sigma_{15}^x) \\ &= (-)(-) (\sigma_7^x \otimes \sigma_{10}^x \otimes \sigma_{11}^x \otimes \sigma_{15}^x) (\sigma_2^z \otimes \sigma_6^z \otimes \sigma_7^z \otimes \sigma_{10}^z) \\ &= C_1 (E_1 B_{p_2}) \end{aligned}$$

$$\begin{aligned} B_{p_6}(C_1 E_1) &= (\sigma_{10}^z \otimes \sigma_{14}^z \otimes \sigma_{15}^z \otimes \sigma_{18}^z) (\sigma_7^x \otimes \sigma_{10}^x \otimes \sigma_{11}^x \otimes \sigma_{15}^x) \\ &= (-)(-) (\sigma_7^x \otimes \sigma_{10}^x \otimes \sigma_{11}^x \otimes \sigma_{15}^x) (\sigma_{10}^z \otimes \sigma_{14}^z \otimes \sigma_{15}^z \otimes \sigma_{18}^z) \\ &= (C_1 E_1) B_{p_6} \end{aligned}$$

So we no longer have any violation in our constrains. We have corrected the error by forming a contractible loop. Note that  $C_1 E_1 = A_{s_7}$  and so it belongs to the stabilizer group, hence acts like the identity on the state. Let us now have a look at the process of the lower diagram. The error occurred is:

$$E_2 = \sigma_{26}^z \sigma_{27}^z \quad (34)$$

giving the state:

$$|\Psi''\rangle = E_2 |\Psi\rangle \quad (35)$$

Both correction schemes (green and red) are of weight 2, so the minimum correcting path rule can't help us here. If we choose the green path  $C_2 E_2 = I$  thus we correct the error completely. Just as easily one can choose the red path  $C'_2$  and here is where the problems begin. By doing so we end up with the operator :

$$C'_2 E_2 = \sigma_{25}^z \otimes \sigma_{26}^z \otimes \sigma_{27}^z \otimes \sigma_{28}^z \quad (36)$$

an operator that commutes with all the "suspicious" stabilizers on vertices  $s_{13,14,15,16}$ . A quick check verify this claim:

$$\begin{aligned} A_{s_{13}}(C'_2 E_2) &= (\sigma_{21}^x \otimes \sigma_{25}^x \otimes \sigma_{28}^x \otimes \sigma_{29}^x) (\sigma_{25}^z \otimes \sigma_{26}^z \otimes \sigma_{27}^z \otimes \sigma_{28}^z) \\ &= (-)(-) (\sigma_{25}^z \otimes \sigma_{26}^z \otimes \sigma_{27}^z \otimes \sigma_{28}^z) (\sigma_{21}^x \otimes \sigma_{25}^x \otimes \sigma_{28}^x \otimes \sigma_{29}^x) \\ &= (C'_2 E_2) A_{s_{13}} \end{aligned}$$

$$\begin{aligned} A_{s_{14}}(C'_2 E_2) &= (\sigma_{22}^x \otimes \sigma_{25}^x \otimes \sigma_{26}^x \otimes \sigma_{30}^x) (\sigma_{25}^z \otimes \sigma_{26}^z \otimes \sigma_{27}^z \otimes \sigma_{28}^z) \\ &= (-)(-) (\sigma_{25}^z \otimes \sigma_{26}^z \otimes \sigma_{27}^z \otimes \sigma_{28}^z) (\sigma_{22}^x \otimes \sigma_{25}^x \otimes \sigma_{26}^x \otimes \sigma_{30}^x) \\ &= (C'_2 E_2) A_{s_{14}} \end{aligned}$$

$$\begin{aligned} A_{s_{15}}(C'_2 E_2) &= (\sigma_{23}^x \otimes \sigma_{26}^x \otimes \sigma_{27}^x \otimes \sigma_{31}^x) (\sigma_{25}^z \otimes \sigma_{26}^z \otimes \sigma_{27}^z \otimes \sigma_{28}^z) \\ &= (-)(-) (\sigma_{25}^z \otimes \sigma_{26}^z \otimes \sigma_{27}^z \otimes \sigma_{28}^z) (\sigma_{23}^x \otimes \sigma_{26}^x \otimes \sigma_{27}^x \otimes \sigma_{31}^x) \\ &= (C'_2 E_2) A_{s_{15}} \end{aligned}$$

$$\begin{aligned}
A_{s_{16}}(C'_2 E_2) &= (\sigma_{24}^x \otimes \sigma_{27}^x \otimes \sigma_{28}^x \otimes \sigma_{32}^x) (\sigma_{25}^z \otimes \sigma_{26}^z \otimes \sigma_{27}^z \otimes \sigma_{28}^z) \\
&= (-)(-)(\sigma_{25}^z \otimes \sigma_{26}^z \otimes \sigma_{27}^z \otimes \sigma_{28}^z) (\sigma_{24}^x \otimes \sigma_{27}^x \otimes \sigma_{28}^x \otimes \sigma_{32}^x) \\
&= (C'_2 E_2) A_{s_{15}}
\end{aligned}$$

Thus we corrected the error but in the process we applied a logical Z operator to one of our encoded qubits. So one would conclude that a bigger lattice will be more error protected. That is not the whole story. We must take in count the error rate. In [8] an error threshold was proven, below which increasing the size of the toric code indeed improves its performance, proving the toric code is a good active error-correcting code. For a more extensive analysis in the subject of error correction on surface codes we recommend [8, 9, 10].

### 3.6 Toric code 2x2 example

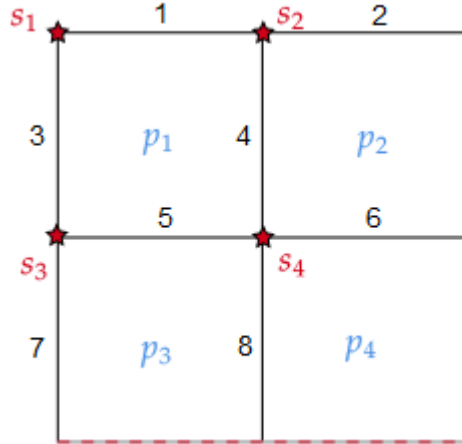


Figure 12:  $2 \times 2$  lattice.

In order to clear some abstruse parts of our theory and to understand the mechanics behind some of our schemes it is deemed necessary to work in an explicit lattice model. As we can see from Figure 12 there are 8 edges, 4

vertices and 4 faces. We can write down the stabilizer operators explicitly:

$$\begin{aligned}
A_{s_1} &= \sigma^x \otimes \sigma^x \otimes \sigma^x \otimes I \otimes I \otimes I \otimes \sigma^x \otimes I \\
A_{s_2} &= \sigma^x \otimes \sigma^x \otimes I \otimes \sigma^x \otimes I \otimes I \otimes I \otimes \sigma^x \\
A_{s_3} &= I \otimes I \otimes \sigma^x \otimes I \otimes \sigma^x \otimes \sigma^x \otimes \sigma^x \otimes I \\
A_{s_4} &= I \otimes I \otimes I \otimes \sigma^x \otimes \sigma^x \otimes \sigma^x \otimes I \otimes \sigma^x \\
B_{p_1} &= \sigma^z \otimes I \otimes \sigma^z \otimes \sigma^z \otimes \sigma^z \otimes I \otimes I \otimes I \\
B_{p_2} &= I \otimes \sigma^z \otimes \sigma^z \otimes \sigma^z \otimes I \otimes \sigma^z \otimes I \otimes I \\
B_{p_3} &= \sigma^z \otimes I \otimes I \otimes I \otimes \sigma^z \otimes I \otimes \sigma^z \otimes \sigma^z \\
B_{p_4} &= I \otimes \sigma^z \otimes I \otimes I \otimes I \otimes \sigma^z \otimes \sigma^z \otimes \sigma^z
\end{aligned} \tag{37}$$

It is obvious that the Hamiltonian of the system:

$$H = - \sum_s A_s - \sum_p B_p \tag{38}$$

is a  $2^8 \times 2^8$  matrix which can be explicitly deduced with the help of Mathematica. According to (16) for this figure, the ground state is (up to a suitable normalization):

$$\begin{aligned}
|\Psi^{(0)}\rangle &= (I + A_{s_1})(I + A_{s_2})(I + A_{s_3})(I + A_{s_4}) |00000000\rangle \\
&= |00000000\rangle + |11100010\rangle + |11010001\rangle + |00110011\rangle \\
&\quad + |00101110\rangle + |11001100\rangle + |11111111\rangle + |00011101\rangle
\end{aligned} \tag{39}$$

As we said before this is not the only ground state. In fact there are three more, linked with the winding number around the different directions of the torus. Meaning that in order to find all the vectors that span the code space we need to act with non contractible loop operators. As it should be clear by now a  $\tilde{Z}$  operator on the primal lattice gives the same state, a  $Z$  operator on the dual lattice and an  $X$  operator on the primal one both take us out of the code space and so we are left with an  $\tilde{X}$  operator on the dual lattice who is just right and will give us the three other states in the code space that we are looking for.

For an odd winding number in the horizontal direction, a number of operators, for example:

$$\sigma_3^x \sigma_4^x, \quad \sigma_7^x \sigma_8^x, \quad \sigma_3^x \sigma_5^x \sigma_8^x \sigma_6^x$$

gives the desirable state:

$$\begin{aligned}
|\Psi^{(1)}\rangle &= \prod_{j=3,4} \sigma_j^x |\Psi^{(0)}\rangle \\
&= |00110000\rangle + |11010010\rangle + |11100001\rangle + |00000011\rangle \\
&\quad + |00011110\rangle + |11111100\rangle + |11001111\rangle + |00101101\rangle
\end{aligned} \tag{40}$$

By a similar logic, any path operator for a closed vertical loop of  $\sigma^x$ , for example :

$$\sigma_1^x \sigma_5^x, \quad \sigma_2^x \sigma_6^x, \quad \sigma_1^x \sigma_4^x \sigma_6^x \sigma_8^x$$

can be acted on  $|\Psi^{(0)}\rangle$  to obtain a new element of the codespace:

$$\begin{aligned}
|\Psi^{(2)}\rangle &= \prod_{j=1,5} \sigma_j^x |\Psi^{(0)}\rangle \\
&= |10001000\rangle + |01101010\rangle + |01011001\rangle + |10111011\rangle \\
&\quad + |10100110\rangle + |01000100\rangle + |01110111\rangle + |10010101\rangle
\end{aligned} \tag{41}$$

While the last of the ground state is given by:

$$\begin{aligned}
|\Psi^{(3)}\rangle &= \prod_{j=1,3,4,5} \sigma_j^x |\Psi^{(0)}\rangle \\
&= |10111000\rangle + |01011010\rangle + |01101001\rangle + |10001011\rangle \\
&\quad + |10010110\rangle + |01110100\rangle + |01000111\rangle + |10100101\rangle
\end{aligned} \tag{42}$$

The energy of these states is  $E = -(P+V) = -8$ . Every pair of anyons gives this energy a boost of +4, considering that each anyon of the pair changes the eigenvalue of a stabilizer operator from +1 to -1. That leads as to the energy spectrum:  $E = -8, -4, 0, +4, +8$ . If we consider the dimension of the Hamiltonian we see that our system is highly degenerate (Figure 13).

As we have seen the toric code can be used to store two logical qubits (regardless the size of the lattice), meaning 4 different logical quantum states by:

$$\begin{aligned}
|00\rangle &= |\Psi^{(0)}\rangle \\
|01\rangle &= |\Psi^{(1)}\rangle \\
|10\rangle &= |\Psi^{(2)}\rangle \\
|11\rangle &= |\Psi^{(3)}\rangle
\end{aligned}$$

where on the left hand side the kets represent logical quantum states and on the right hand side the states are of the noisy, physical, quantum spin

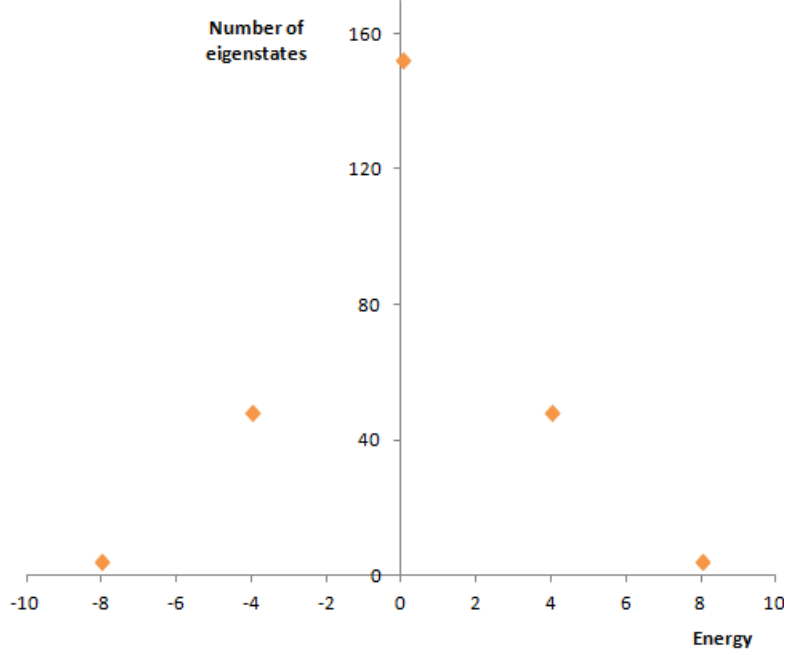


Figure 13: Degeneracy of the energy spectrum of toric code in Figure 9.

lattice.

Let us now verify our previous section statement about the logical  $\tilde{Z}$  and  $\tilde{X}$  operators. Remember we claimed that the creation of pairs of anyons, the transportation of one around the torus and the annihilation of the pair equals with the action of a logical Pauli operator on one of our logical qubits. More precisely in our case we have for the first logical qubit:

$$\tilde{X}_1 = \prod_{j=1,5} \sigma_j^x, \quad \tilde{Z}_1 = \prod_{j=1,2} \sigma_j^z \quad (43)$$

while for the second:

$$\tilde{X}_2 = \prod_{j=3,4} \sigma_j^x, \quad \tilde{Z}_2 = \prod_{j=3,7} \sigma_j^z \quad (44)$$

It is obvious due to the overlap of our operators in exactly one edge that:

$$\tilde{X}_1 \tilde{Z}_1 = -\tilde{Z}_1 \tilde{X}_1, \quad \tilde{X}_2 \tilde{Z}_2 = -\tilde{Z}_2 \tilde{X}_2 \quad (45)$$

As it is also obvious that any other combination commutes.

We are now ready to see the action of these operators on our encoded states (to be frank we already have seen some (eq.40-42) but let's see it with a formalism that will make our point crystal clear):

$$\begin{aligned}
\tilde{X}_1 |00\rangle &= \prod_{j=1,5} \sigma_j^x |\Psi^{(0)}\rangle = |\Psi^{(2)}\rangle = |10\rangle \\
\tilde{X}_1 |01\rangle &= \prod_{j=1,5} \sigma_j^x |\Psi^{(1)}\rangle = |\Psi^{(3)}\rangle = |11\rangle \\
\tilde{X}_1 |10\rangle &= \prod_{j=1,5} \sigma_j^x |\Psi^{(2)}\rangle = |\Psi^{(0)}\rangle = |00\rangle \\
\tilde{X}_1 |11\rangle &= \prod_{j=1,5} \sigma_j^x |\Psi^{(3)}\rangle = |\Psi^{(1)}\rangle = |01\rangle \\
\tilde{Z}_1 |00\rangle &= \prod_{j=1,2} \sigma_j^z |\Psi^{(0)}\rangle = |\Psi^{(0)}\rangle = |00\rangle \\
\tilde{Z}_1 |01\rangle &= \prod_{j=1,2} \sigma_j^z |\Psi^{(1)}\rangle = |\Psi^{(1)}\rangle = |01\rangle \\
\tilde{Z}_1 |10\rangle &= \prod_{j=1,2} \sigma_j^z |\Psi^{(2)}\rangle = -|\Psi^{(2)}\rangle = -|10\rangle \\
\tilde{Z}_1 |11\rangle &= \prod_{j=1,2} \sigma_j^z |\Psi^{(3)}\rangle = -|\Psi^{(3)}\rangle = -|11\rangle
\end{aligned} \tag{46}$$

Accordingly for the second logical qubit:

$$\begin{aligned}
\tilde{X}_2 |00\rangle &= \prod_{j=3,4} \sigma_j^x |\Psi^{(0)}\rangle = |\Psi^{(1)}\rangle = |01\rangle \\
\tilde{X}_2 |01\rangle &= \prod_{j=3,4} \sigma_j^x |\Psi^{(1)}\rangle = |\Psi^{(0)}\rangle = |00\rangle \\
\tilde{X}_2 |10\rangle &= \prod_{j=3,4} \sigma_j^x |\Psi^{(2)}\rangle = |\Psi^{(3)}\rangle = |11\rangle \\
\tilde{X}_2 |11\rangle &= \prod_{j=3,4} \sigma_j^x |\Psi^{(3)}\rangle = |\Psi^{(2)}\rangle = |10\rangle \\
\tilde{Z}_2 |00\rangle &= \prod_{j=3,7} \sigma_j^z |\Psi^{(0)}\rangle = |\Psi^{(0)}\rangle = |00\rangle \\
\tilde{Z}_2 |01\rangle &= \prod_{j=3,7} \sigma_j^z |\Psi^{(1)}\rangle = -|\Psi^{(1)}\rangle = -|01\rangle \\
\tilde{Z}_2 |10\rangle &= \prod_{j=3,7} \sigma_j^z |\Psi^{(2)}\rangle = |\Psi^{(2)}\rangle = |10\rangle \\
\tilde{Z}_2 |11\rangle &= \prod_{j=3,7} \sigma_j^z |\Psi^{(3)}\rangle = -|\Psi^{(3)}\rangle = -|11\rangle
\end{aligned} \tag{47}$$

From (46),(47) it becomes clear that the operators we are talking about are the logical Pauli X,Z for each encoded qubit. Unfortunately these are two very simple quantum gates, the Not gate and the phase flip gate accordingly, which do not meet the criteria for universal quantum computing.

It is obvious that our toy model would do awful as a fault tolerant system due to its small size. Following the error correcting procedure that has been employed earlier we see that even after one rotational error the risk to perform a logical operation to our qubits in our attempt to correct that error is really high.

## 4 $\mathbb{Z}_d$ Kitaev model

Taking one step further away from the trivial case we introduce in this section the  $\mathbb{Z}_d$  Kitaev model which is a generalization of the Kitaev model from  $\mathbb{Z}_2$  group ( toric code ) to  $\mathbb{Z}_d$  group. The model is again defined on a square lattice with periodic boundary conditions, although any 2- dimensional lattice would do. The sole difference from before is that instead of placing a qubit on each edge, we place a qudit (d-level system). We will first



derive a general theory for qudits [11, 12, 13] and then consider the  $d = 5$  case (References 12, 13 focus their attention to  $\mathbb{Z}_3$ ).

Same as before the Hamiltonian of the model consists of two kind of operators, i.e the vertex and the plaquette operators. These operators are define based on the generalized Pauli operators acting on a qudit as:

$$X |j\rangle = |j + 1 \bmod d\rangle, \quad Z |j\rangle = \omega^j |j\rangle \quad (48)$$

Where due to the cyclic notation of our operators (actually the symmetry of  $\mathbb{Z}_d$  group) :  $Z^d = X^d = I_d$ , we have that  $\omega$  is the  $d$ -th root of unity:

$$\omega = e^{2\pi i/d} \quad (49)$$

Additionally it is easy to verify from (48) the commutation relation between these two operators:

$$ZX = \omega XZ \quad (50)$$

For general  $d$  the eigenvalues of  $X, Z$  which are going to help us construct the stabilizer group generators of our new model, lie within the unit circle so that  $+1$  is still (as in toric code) the max possible value.

The Hamiltonian of our system is given by the familiar sum of the plaquettes and vertex operators as:

$$H = - \sum_s A_s - \sum_p B_p \quad (51)$$

In order for the model to be exactly solvable remember that the  $A_s$ 's and  $B_p$ 's are defined such that they commute with each other. Note that a definition as before won't cut it, and that is because although  $[A_s, B_p] = 0$  when the two operators share no common edge, when they have two edges in common (recall that this is the only other option) it is easy to see that their commutator becomes:

$$[A_s, B_p] = (1 - \omega^2) A_s B_p \quad (52)$$

which is zero when  $d = 2$  because then  $\omega^2 = 1$  but not when  $d > 2$ .

To this end we assign an orientation to our lattice and define the  $A_s$  and  $B_p$  as follows.

For the vertex operator we have:

$$A_s = \prod_{j \in \text{star}(s)} X_j^{\pm 1} \quad (53)$$

where  $X_j^{-1}$  is used if an arrow points towards vertex  $j$ , otherwise we use  $X_j$ . While for the plaquette operator:

$$B_p = \prod_{j \in \text{boundary}(p)} Z_j^{\pm 1} \quad (54)$$

where we take an anti-clockwise route around the edges that consists the boundary of the plaquette and use the  $Z_j$  when an edge has the same orientation as the route, otherwise we use  $Z_j^{-1}$ . We note that this definition for our stabilizer codes leads to a non hermitian Hamiltonian, a problem that will easily get fixed with the addition of the hermitian conjugate Hamiltonian.

Let us take a moment to prove our claim, i.e to prove that the operators we just constructed commutes with each other.

Following Figure 14 we have:

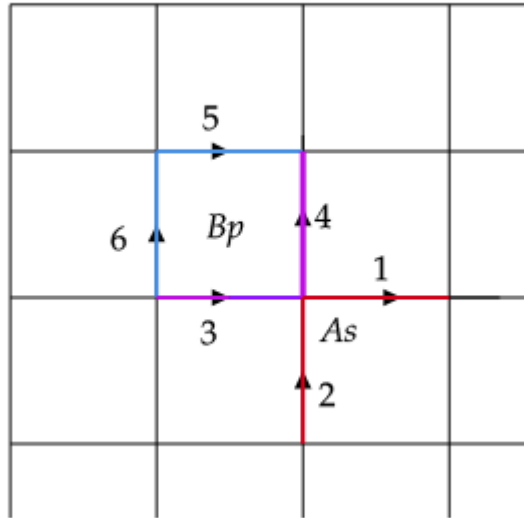


Figure 14: Stabilizer operators overlap on two edges.

$$[A_s, B_p] = A_s B_p - B_p A_s$$

Where:

$$\begin{aligned} B_p A_s &= (Z_3 \otimes Z_4 \otimes Z_5^{-1} \otimes Z_6^{-1})(X_1 \otimes X_2^{-1} \otimes X_3^{-1} \otimes X_4) \\ &= \omega^{-1} \omega A_s B_p = A_s B_p \end{aligned}$$

So we derive  $[A_s, B_p] = 0$ .

Note that in this model too, there are  $2k^2$  stabilizer generators in the Hamiltonian, but only  $2k^2 - 2$  of them are independent, because of the following two constrains:

$$\prod_s A_s = \prod_p B_p = I$$

So there are  $d^2$  degenerate ground states.

As we have seen before the ground states are the states that are stabilized by all of the vertex and plaquette operators simultaneously. We start with the state:

$$|\tilde{0}\tilde{0}\rangle = \prod_s (I + A_s + A_s^2 + \dots + A_s^{d-1}) |0\rangle^{\otimes n} \quad (55)$$

For the other  $d^2 - 1$  degenerate ground states let's first define the logical operators for our qudits in an analogues manner with the toric code:

- $\tilde{Z}_1 = \prod_{j \in c_{z1}} Z^{\pm 1}$  where  $c_{z1}$  is a horizontal loop on the torus. We act to an edge with  $Z$  if the edge's direction is the same as moving's direction, otherwise we act with  $Z^{-1}$ .
- $\tilde{Z}_2 = \prod_{j \in c_{z2}} Z^{\pm 1}$  where  $c_{z2}$  is a vertical loop on the torus. We act to an edge with  $Z$  if the edge's direction is the same as moving's direction, otherwise we act with  $Z^{-1}$ .
- $\tilde{X}_1 = \prod_{j \in c_{x1}} X^{\pm 1}$  where  $c_{x1}$  is a vertical loop on the torus (this time on the dual lattice). We act to an edge with  $X$  if the edge's direction is the same as moving's direction, otherwise we act with  $X^{-1}$ .
- $\tilde{X}_2 = \prod_{j \in c_{x2}} X^{\pm 1}$  where  $c_{x2}$  is a horizontal loop on the torus (again on dual lattice). We act to an edge with  $X$  if the edge's direction is the same as moving's direction, otherwise we act with  $X^{-1}$ .

So the other ground states are:

$$|\tilde{i}\tilde{j}\rangle = \tilde{X}_2^j \tilde{X}_1^i |\tilde{0}\tilde{0}\rangle, \quad i, j = 0, 1, 2, \dots, d-1 \quad (56)$$

It is also true that:

$$\tilde{Z}_1 |\tilde{i}\tilde{j}\rangle = \omega^i |\tilde{i}\tilde{j}\rangle, \quad \tilde{Z}_2 |\tilde{i}\tilde{j}\rangle = \omega^j |\tilde{i}\tilde{j}\rangle \quad (57)$$

This is an analogues scheme with the one we used in toric code with the difference that here we have embed the possibility of creating and moving different types of plaquette anyons, leading to different ground states. We will get a better grip on that concept after the next section.

#### 4.1 Anyon model

The theory developed above was done for the general case of qudits. From now on we will focus on the case where  $d=5$ . We need to compute the energy gap of the Hamiltonian, i.e. the energy difference between the ground state where the code lies and the excited states which represent the errors. It is also important to calculate the anyon statistics, as long as they are associated with the excitations of a topological system with qudits.

At  $d = 5$  we choose the base:

$$|0\rangle, |1\rangle, |2\rangle, |3\rangle, |4\rangle$$

that span the Hilbert space of a qudit. The action of the generalized Pauli operators on this basis is given according to eq. 48 by:

$$X |0\rangle = |1\rangle, \quad X |1\rangle = |2\rangle, \quad X |2\rangle = |3\rangle, \quad X |3\rangle = |4\rangle, \quad X |4\rangle = |0\rangle$$

$$Z |0\rangle = |0\rangle, \quad Z |1\rangle = \omega |1\rangle, \quad Z |2\rangle = \omega^2 |2\rangle, \quad Z |3\rangle = \omega^3 |3\rangle, \quad Z |4\rangle = \omega^4 |4\rangle$$

which gives the following matrices:

$$X = \begin{pmatrix} 0 & 0 & 0 & 0 & 1 \\ 1 & 0 & 0 & 0 & 0 \\ 0 & 1 & 0 & 0 & 0 \\ 0 & 0 & 1 & 0 & 0 \\ 0 & 0 & 0 & 1 & 0 \end{pmatrix}, \quad Z = \begin{pmatrix} 1 & 0 & 0 & 0 & 0 \\ 0 & \omega & 0 & 0 & 0 \\ 0 & 0 & \omega^2 & 0 & 0 \\ 0 & 0 & 0 & \omega^3 & 0 \\ 0 & 0 & 0 & 0 & \omega^4 \end{pmatrix} \quad (58)$$

where  $\omega = e^{2\pi i/5}$ .

From (eq. 58) it is straightforward to see that  $X, Z$  are not hermitian, that

$X^5 = Z^5 = I_5$  and that both  $X, Z$  have eigenvalues  $\omega^g$ ,  $g = 0, 1, 2, 3, 4$  or more explicitly:

$$\omega^0 = 1, \quad \omega = e^{2\pi i/5}, \quad \omega^2 = e^{4\pi i/5}, \quad \omega^3 = -e^{\pi i/5}, \quad \omega^4 = -e^{3\pi i/5} \quad (59)$$

It is obvious from the definition of the stabilizer operators that  $A_s$  and  $B_p$  has  $\omega^g$  as their eigenvalues too. As we said before  $\omega = e^{2\pi i/5}$  is the 5-th root of unity so 1 is the maximum eigenvalue and the ground state space is defined by the same constrains as in toric code, namely:

$$A_s |\Psi\rangle = |\Psi\rangle, \quad B_p |\Psi\rangle = |\Psi\rangle \quad \forall s, p$$

Errors on the system can be expressed in terms of operators  $X, Z$  or products containing them, and acting on each edge  $j$  where the qudits are placed. To see what effect these errors have on the system, we will see how the ground state changes by applying  $X, Z$ . We will see that this corresponds to processes in which anyons are created, annihilated or moved throughout the torus, in a completely analogues way as in the previous model. Let's see what happens if we act on a ground state with operator  $Z_j$ :

$$|\Psi'\rangle = Z_j |\Psi\rangle$$

As it has to be clear by now this operation leads to the violation of the two vertex constrains that are involved with the  $j$ -th edge. The difference with the  $d = 2$  case is that now there is an orientation on our lattice leading to different eigenvalues on each involved vertex, i.e different kind of violation, so different anyons. Let's see an example. From now on consider a lattice whose horizontal edges point to the right while its vertical edges points up (Figure 15a). For the left vertex ( $s$ ) we have:

$$\begin{aligned} A_s Z_j |\Psi\rangle &= (X_j \otimes X_k \otimes X_l^{-1} \otimes X_m^{-1})(Z_j \otimes I_k \otimes I_l \otimes I_m) |\Psi\rangle \\ &= \omega^{-1} Z_j A_s |\Psi\rangle = \omega^{-1} |\Psi'\rangle = \omega^4 |\Psi'\rangle \end{aligned} \quad (60)$$

where the  $I$ 's of the non correlated qudits were omitted for convenience. For the right vertex ( $s'$ ) we get:

$$\begin{aligned} A_{s'} Z_j |\Psi\rangle &= (X_p \otimes X_q \otimes X_j^{-1} \otimes X_r^{-1})(I_p \otimes I_q \otimes Z_j \otimes I_r) |\Psi\rangle \\ &= \omega Z_j A_{s'} |\Psi\rangle = \omega |\Psi'\rangle \end{aligned} \quad (61)$$

To these violations we attach two different vertex anyons,  $e^{-1}$  (i will use this notation rather than  $e^4$  to make the particle antiparticle interpretation easier

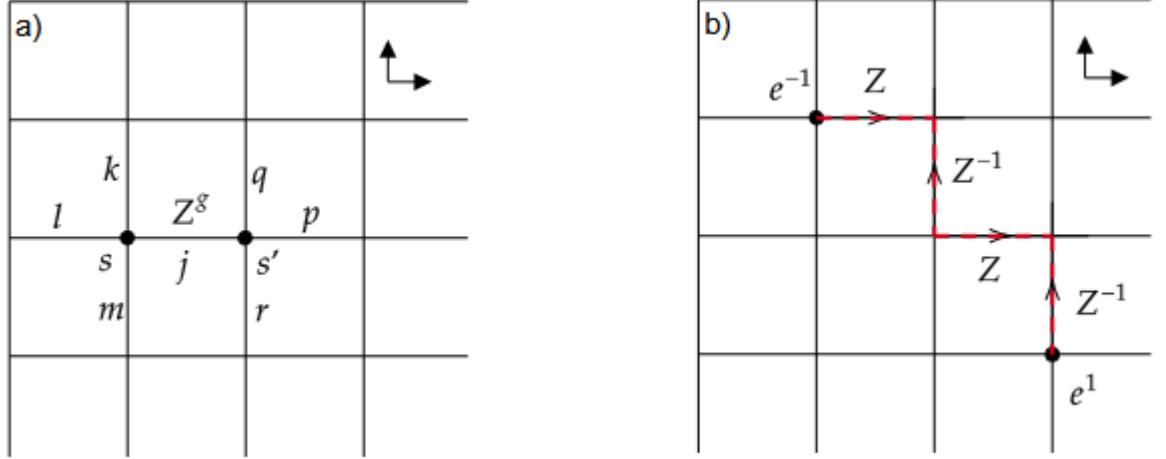
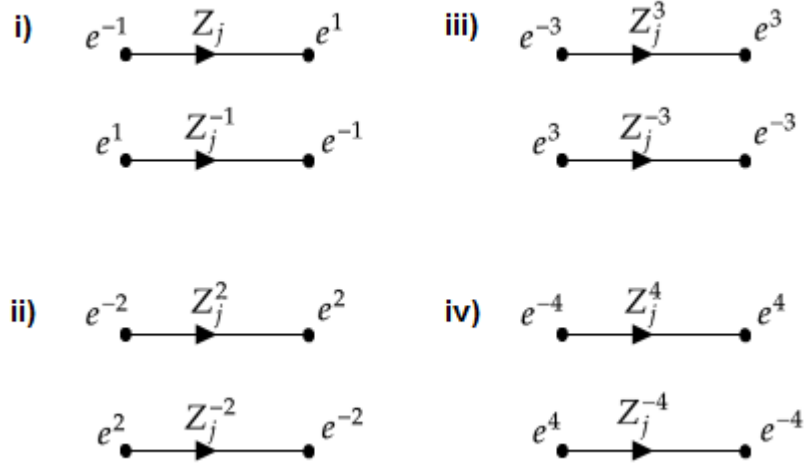


Figure 15: a) We are acting with a  $Z^g$  rotation on the  $j$ -th edge, leading to violation in constraints for  $s, s'$  vertices. b) We are moving an  $e^1$  anyon through the lattice using suitable operators to cope with the orientation of the edges.

for the eye) and  $e^1$  accordingly. We notice that in this case the anyons are not antiparticles to themselves but rather the  $e^g$  anyon has the  $e^{-g} = e^{d-g}$  as antiparticle. This has to do with the symmetry of the group we use. What happens if we act on the  $j$ -th edge with  $Z_j$  again? After we convince ourselves about  $Z^a X^b = \omega^{ab} X^b Z^a$  it is easy to see:

$$\begin{aligned} A_{s'} Z_j^2 |\Psi\rangle &= \omega^{-2} Z_j^2 A_s |\Psi\rangle = \omega^{-2} |\Psi'\rangle \\ A_s Z_j^2 |\Psi\rangle &= \omega^2 Z_j^2 A_{s'} |\Psi\rangle = \omega^2 |\Psi'\rangle \end{aligned} \quad (62)$$

giving birth to the  $e^{-2}, e^2$  pair of vertex anyons. If we keep on going we derive all the vertex charges of our model. We sum the procedure of the vertex anyons creation into the following schematic rules:



Notice that if we want to create a pair with opposite orientation than the one we described above it suffices to act on the desired edge with the inverse operator. That gives us a tool to move an anyon around with respect to the orientation of the lattice (Figure 15b) (more on this in the fusion section). It is important to point out once more that  $e^{-g}$  does not define new anyons because as we already mentioned  $\omega^{-g} = \omega^{d-g} = \omega^{g'}$  where  $g, g' = 0, 1, \dots, 4$ . Once again it is exactly analogous to construct the creation process for the plaquette anyons. The only thing we need to be aware of is the orientation of the dual lattice. Since it is made from the  $\pi/2$  rotation of the primal lattice, it has its horizontal edges point to the left and its vertical ones point up (we choose a counter clockwise rotation).

## 4.2 Fusion process

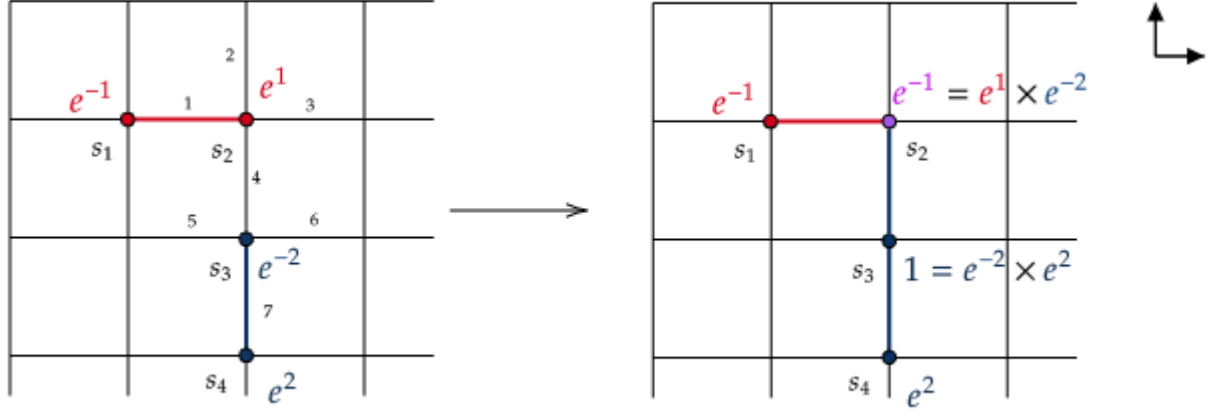


Figure 16: Fusion process of two e-type anyons

We begin with the categorisation of our abelian anyons:

$$1, e^g, m^h, \epsilon^{g,h} \text{ for } g, h = 0, 1, \dots, 4 \quad (63)$$

where 1 denotes again the absence of an anyon of any kind and  $\epsilon^{g,h}$  denotes the combination of  $e^g$  and  $m^h$  anyons. So the number of different types of anyons of our model is  $d^2 = 25$ .

The fusion rules are given by:

$$e^g \times e^h = e^{(g+h) \bmod 5}, \quad m^g \times m^h = m^{(g+h) \bmod 5}, \quad e^g \times m^h = \epsilon^{g,h} \quad (64)$$

Any other combination can be deduced by these three rules, the fact that our anyons are abelian and the structure of the  $\epsilon$ . Let's be a little more analytic about what the above operations mean. Take for example Figure 16. We begin by acting with the operators  $Z_1$  and  $Z_7^{-2}$  on a state  $|\Psi\rangle$ , thus:

$$|\Psi'\rangle = Z_1 Z_7^{-2} |\Psi\rangle \quad (65)$$

Figure 16 illustrates the creation of the vertex anyons as indicated by the schematic rules we derived earlier. What will happen if we act with  $Z_4^{-2}$ ?



It is obvious that the involved vertices are being occupied by two anyons (each) leading to their fusion, that is  $s_2 : e^1 \times e^{-2}$  and  $s_3 : e^{-2} \times e^2$ . Let's verify the fusion rules by calculating the constrains in question:

$$\begin{aligned}
A_{s_2} Z_4^{-2} Z_1 Z_7^{-2} |\Psi\rangle &= (X_1^{-1} X_2 X_3 X_4^{-1}) (Z_1 Z_4^{-2} Z_7^{-2}) |\Psi\rangle \\
&= \omega^1 \omega^{-2} (Z_1 Z_4^{-2} Z_7^{-2}) (X_1^{-1} X_2 X_3 X_4^{-1}) |\Psi\rangle \quad (66) \\
&= \omega^{-1} (Z_1 Z_4^{-2} Z_7^{-2}) |\Psi\rangle
\end{aligned}$$

But this means we got an anyon  $e^{-1}$  in the vertex  $s_2$  and thus the respective fusion rule holds. As we see the fusion rules are nothing more than a corollary of the product of the eigenvalues of our stabilizers and the cyclic notation they accumulate for being roots of unity. For thoroughness lets see the other vertex:

$$\begin{aligned}
A_{s_3} Z_4^{-2} Z_1 Z_7^{-2} |\Psi\rangle &= (X_4 X_5^{-1} X_6 X_7^{-1}) (Z_1 Z_4^{-2} Z_7^{-2}) |\Psi\rangle \\
&= \omega^2 \omega^{-2} (Z_1 Z_4^{-2} Z_7^{-2}) (X_4 X_5^{-1} X_6 X_7^{-1}) |\Psi\rangle \quad (67) \\
&= (Z_1 Z_4^{-2} Z_7^{-2}) |\Psi\rangle
\end{aligned}$$

In this case we see that we end up with no anyon at all. That is because  $e^{-2}$  is the antiparticle of  $e^2$  and they fuse to annihilation. This convenience of spotting ones antiparticle is the reason we keep the  $e^{-g}$  symbolism although, as we have already made clear, the right one is  $e^{d-g}$ . On this last procedure exactly lies the scheme we use to move an anyon around the lattice. We have to act with the suitable operators that annihilate the anyon in question from the one endpoint of an edge (by creating there its antiparticle) and reappear it on the other endpoint of that same edge. It is obvious that in complete analogy with the toric code, the anyonic charge in this model is preserved modulo 5 ( $\mathbb{Z}_5$  symmetry).

### 4.3 Anyon statistics

Let us now study the braiding of the anyons. First we note that the exchange of identical  $e^g$  ( $m^h$ ) anyons leads to the creation of a contractible loop with no effect on our wave function (exactly as in toric code). Thus once again the mutual statistics of  $e^g$  and  $m^h$  is that of bosons.

The braiding of an  $e^g$  anyon around a  $m^h$  anyon is shown in Figure 17. With

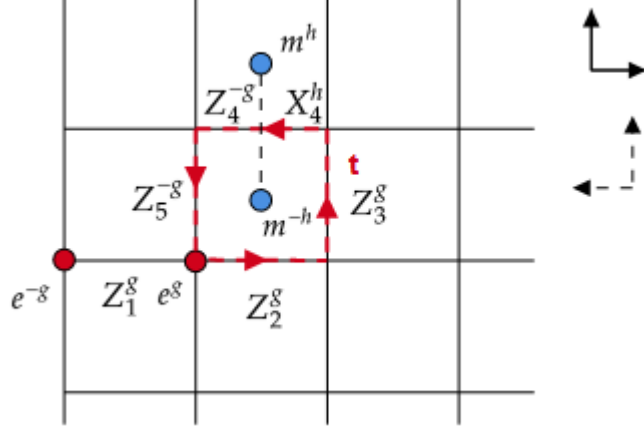


Figure 17:  $e^g, m^h$  braiding

the experience we have gained so far we can see:

$$\begin{aligned}
|\Psi_{in}\rangle &= Z_1^g X_4^h |\Psi\rangle \\
|\Psi_{fin}\rangle &= S_z^g(t) Z_1^g X_4^h |\Psi\rangle \\
&= \left( Z_2^g Z_3^g Z_4^{-g} Z_5^{-g} \right) Z_1^g X_4^h |\Psi\rangle \\
&= \omega^{-gh} Z_1^g X_4^h \left( Z_2^g Z_3^g Z_4^{-g} Z_5^{-g} \right) |\Psi\rangle \\
&= \omega^{-gh} Z_1^g X_4^h |\Psi\rangle = \omega^{-gh} |\Psi_{in}\rangle
\end{aligned} \tag{68}$$

Where in the last line, for one more time, we used the fact that a contractible loop does not affect our state.

So in the qudit case too we have anyonic behaviour when braiding  $e$  with  $m$  type anyons. As it is clear, this model gives us a much richer statistics than the toric code due to the large variance of anyons and so a bit more complex quantum gates (through braiding), gates that in this case too are not enough for universal computing (a generalised logical X, Z Pauli). It is also important to note that a clockwise braiding would lead to different results, a concept unknown until now.

With a similar argument as in the previous section we deduce the phase of a dyon exchange by rotating it by  $2\pi$  around itself (counter clockwise). This is similar as the braiding between  $e^g$  and  $m^h$  giving a phase of  $\omega^{gh}$ . Lastly we check the braiding of the dyon  $(g,h)$  around the dyon  $(g',h')$ .

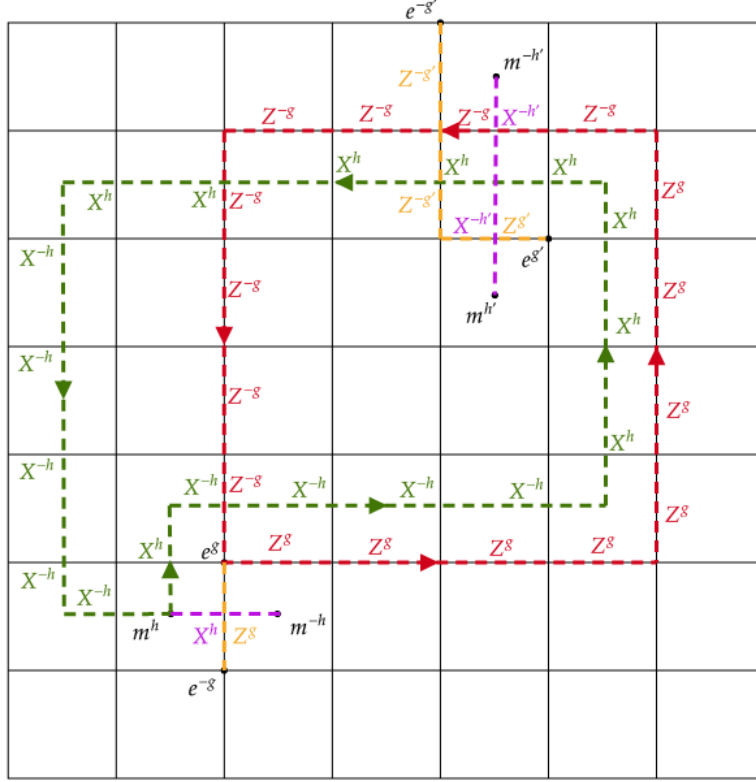


Figure 18: Dyon braiding process

According to Figure 18 a non trivial phase is accumulated under the action of braid because the closed loop string operators that wind  $(g, h)$  collide with the strings connecting the dyon  $(g', h')$  with its antiparticle. At the two locations of intersection we have:

$$Z^{-g} X^{-h'} = \omega^{gh'} X^{-h'} Z^{-g}, \quad X^h Z^{-g'} = \omega^{hg'} Z^{-g'} X^h \quad (69)$$

giving an overall phase of  $\omega^{gh'+hg'}$ .

To sum up our findings it is useful to introduce the R-matrix or exchange matrix, which when talking about abelian anyons is the global phase that our system acquires after exchange procedures take place. In contrast, exchange statistics of non Abelian anyons leads to the implementation of unitary operators, making them far more appealing for quantum computation.  $R^2$  is the braid matrix for the abelian case. Note that for non-abelian anyons

the different possible outcomes from fusion must be concerned when talking about braiding ( $B = F^\dagger R^2 F$ ), where F-matrix indicates the base change between the different fusion channels [29]. As our abelian anyons have only one fusion channel the fusion matrix is trivial and thus Braid matrix coincides with  $R^2$ .

$$R_{e^g e^h}^{e^{g+h}} = R_{m^g m^h}^{m^{g+h}} = I, \quad \left(R_{e^g m^h}^{e^{g+h}}\right)^2 = \omega^{gh}, \quad R_{e^g, h_{e^g, h}}^{e^{g+g}, h+h} = \omega^{gh}, \quad R_{e^g, h_{e^g, h'}}^{e^{g+g'}, h+h'} = \omega^{gh'+h'g}$$

#### 4.4 Excitation Energy

Let us look at the gap of the Hamiltonian. Remember that in order for our Hamiltonian to be hermitian we take:

$$H_{tot} = \frac{1}{2}[H + H^\dagger] \quad (70)$$

So for the ground state we have:

$$H_{tot} |\Psi\rangle = \frac{1}{2} \left( - \sum_s A_s - \sum_p B_p - h.c \right) |\Psi\rangle = -(V + P) |\Psi\rangle \quad (71)$$

While for a state with a pair of vertex anyon on the limits of the j-th edge (s, s') we have:

$$\begin{aligned} H_{tot} Z_j^g |\Psi\rangle &= \frac{1}{2} \left( - \sum_s A_s - \sum_p B_p - h.c \right) Z_j^g |\Psi\rangle \\ &= -(V + P - 2) Z_j^g |\Psi\rangle - \frac{1}{2} (A_s + A_{s'} + A_s^\dagger + A_{s'}^\dagger) Z_j^g |\Psi\rangle \\ &= -(V + P - 2) Z_j^g |\Psi\rangle - \frac{1}{2} (\omega^{-g} + \omega^g + \omega^g + \omega^{-g}) Z_j^g |\Psi\rangle \quad (72) \\ &= -(V + P - 2 + \omega^{-g} + \omega^g) Z_j^g |\Psi\rangle \\ &= -(V + P - 2 + e^{-\frac{2g\pi i}{5}} + e^{\frac{2g\pi i}{5}}) Z_j^g |\Psi\rangle \\ &= - \left( V + P - 2 + 2 \cos \left( \frac{2g\pi}{5} \right) \right) Z_j^g |\Psi\rangle \end{aligned}$$

Thus the energy difference is:

$$\Delta E = 2 - 2 \cos \left( \frac{2g\pi}{5} \right) \quad (73)$$

The action of X produces the same energy increment but we have to do the commutation with the operators  $B_p$ . We note that there is a reduction of

the energy gap in comparison with the qubit case ( $\Delta E = 4$ ). As before it is clear that the movement of the pair of anyons through the lattice does not cost any additional energy to the system.

In the case of  $d = 5$  we have the completely new process of fusing vertex (plaquette) anyons together to form a new anyon rather than annihilate them (see eq. 64). Let's see how this process reflects to the energy scheme. Assume we have two pairs of vertex anyons, namely  $(e^{-g}, e^g)$  and  $(e^{-h}, e^h)$ . The energy of that state is:

$$E_1 = - \left( V + P - 4 + 2\cos\left(\frac{2g\pi}{5}\right) + 2\cos\left(\frac{2h\pi}{5}\right) \right)$$

Now assume that we bring  $e^g$  and  $e^{-h}$  together. By the fusion rules we get:

$$e^g \times e^{-h} = e^{(g-h) \bmod 5}$$

The new state has energy:

$$E_2 = - \left( V + P - 3 + \cos\left(\frac{2g\pi}{5}\right) + \cos\left(\frac{2h\pi}{5}\right) + \cos\left(\frac{2[(g-h) \bmod 5]\pi}{5}\right) \right)$$

It will be useful to take a specific example to make our conclusions clearer (check Figure 16). Let's take  $g = 1$  and  $h = 2$ . That leaves us with:

$$\Delta E = E_1 - E_2 \simeq 1.8 \tag{74}$$

What has occurred is that two anyons have been tied together, but not annihilated. This process lowers the energy of the system by a smaller amount than the process of annihilation.

The error correction process for this model is similar with that of the toric code with one notable difference. Remember that in toric we had absolutely no idea of the error chain. The only thing we knew for sure was the place of the errors (anyons). Although this is fundamental to the construction of an ECC and is true in principle to the generalised model too, the difference lies in the fact that due to the possibility of two anyons fuse together to something different than the vacuum, it is possible to have clues for the certain error chain that occurred.

## 5 Topological quantum memory

Models with abelian anyons as the ones analysed in this work are suitable candidates to realize a d-dimensional topological quantum memory, e.g a

system to safely store quantum information. A system like that should meet certain criteria, called the Caltech rules and presented in [14] as:

- (finite spins) It consists of finite dimensional spins embedded in  $R^d$  with finite density.
- (bounded local interactions) It evolves under a Hamiltonian comprised of a finite density of interactions of bounded strength and bounded range.
- (nontrivial codespace) It encodes at least one qubit in its degenerate ground space.
- (perturbative stability) The logical space associated with at least one encoded qubit must be perturbatively stable in the thermodynamic limit.
- (efficient decoding) This encoded qubit allows for a polynomial time decoding algorithm.

The first three of these criteria are being satisfied by the Kitaev models by construction. As of the stability, the analysis proceeding this section shows that our models are robust against local errors and as a matter of fact against global errors consisting of a number of local errors too, through the active correcting procedure we presented in 3.4 . The stability under perturbations was shown in [15]. In relation with the last bullet generally speaking the aim of a decoding algorithm is to use the information given by the syndrome to return a correction operator that restores the code to its original state. As we already mentioned it has been found in [8] an error rate threshold under which increasing the size of the toric code increases its error correcting performance. With all that we conclude that toric code is an efficient active correcting code that can serve reliable as a quantum memory. By active we mean one that needs external help to be reliable. A scheme of how we can encode logical qubits in the toric architecture is given in [16, 17]

## 5.1 Further work

After all this analysis we conclude that our models are not ideal, to say the least. A lot of work has been done since these first steps towards the realisation of a truly fault tolerant quantum computer, a work that led to more optimal models for this job.

Let's pretend for a minute we care only for the fault tolerant storage of information. Although as we said our models are good candidates for this task a truly robust quantum memory would be one in which the lifetime of the encoded qubits would scale with the number of the physical ones. A device like that is called a passive correcting quantum memory or more commonly a self-correcting quantum memory because it wouldn't need any external procedure to stay stable (the error correcting procedure would still be necessary for the encoding and measurements parts but not for the "waiting" period). More specifically such a construction would require the accumulation of error excitations over time, which can in turn lead to logical errors, to be energetically disfavoured due to the presence of a macroscopic energy barrier. By this we mean that the minimum energy needed to take the system from a code state to an orthogonal one, thus realize a logical error (by means of a sequence of local errors), should be scaled with the number of physical qudits. Unfortunately there has been proved a no-go theorem for a two-dimensional self-correcting quantum memory based on stabilizer codes [18]. A kind of sloppy argument for this is that in both toric code and the generalised Kitaev model the energy barrier is constant. Remember the only energy we need is that of creating a pair of anyons (gap of the ground state). From there on to move them around the torus costs no energy and to annihilate them is energetically preferable. Further analysis of this exceeds the scope of this work but can be found in [19], [20]. A lot of work has been made in the front of realizing such a system. Some of the models with this quality are the 4D toric code on a cubic lattice [8, 21], symmetry protected 3D spin lattice models [22] or even 2D toric code with effective long-range interactions between its anyonic excitations [23].

Now let's trouble ourselves with the problem of processing the information, atop that of storage. Our models as we have already seen cannot realize universal quantum computing because they cannot realize universal quantum gates (a set of gates that can approximate any unitary transformation), a fact that seems to make them inappropriate for the task. The top candidates for these job, as we already mentioned, are models that has non-Abelian anyons as excitations. In this models the information is encoded into the excitation spectrum. In contrast to abelian anyons the non-abelian ones have a fusion space of non trivial multiplicity, the orthogonal states of which can encode the logical qubits. But we don't throw the towel on abelian anyons and their capability for universal quantum computation just yet. The much easier experimental realization [24, 25, 26] in compare with

the non-Abelian ones [27] makes it charming if not demanding to find ways to make this work. And so it has, by supplement our models with non-topological operations (thus not so error resistant). Either by introducing magic state distillation [28] or by single spin measurements [29], through the planar code, which is a variation of the toric code with a more feasible geometric structure and some other comforts [8], we can achieve universality.

## 6 Conclusion

To sum up we started our work reasoning why the realization of a fault tolerant quantum computer is of high interest. We described the key points behind the error correcting code theory which is the theory burdened with the responsibility to deal with the problems that make our venture so challenging, i.e the noise that renders our systems unstable. We focused our analysis on Kitaev's toric code, the first quantum error correcting code that confronted the problem of error robustness at the physical level. More specifically we saw that the quantum information can be encoded in the degenerate ground space of a multi-qubit system rendering it inaccessible to local operations. The excitations of a system like that turns out to be anyonic quasi-particles the braiding of which realizes quantum gates. Due to the abelian nature of our anyons we could only realize two too simple gates the NOT gate and the Phase flip one. Moreover we introduced an error correction procedure which applies to our system externally to deal with the accumulation of local errors into global ones (logical errors) over time. Next we move on to a generalised Kitaev lattice model, the building blocks of which are 5-level systems. Following the same analysis as before we see that new abelian anyons arise with novel braiding properties, i.e new, richer statistics by exchanging particles. Furthermore new energy processes appear which are forbidden for qubits. Except from the obvious advantage of larger capacity for information storage and greater potential generalised models have in relation with quantum information processing (although again not forming a universal set of gates), it is important to see if they are better at suppressing the logical errors. As a matter of fact [30] shows that the more complex energy landscape of  $Z_5$  accomplishes through entropic suppression just that. We conclude our work by discussing ways to overcome the limitations of our models regarding either their capability of information safe storage or their inefficiency to produce a universal set of gates, by directing the interested reader to the relative literature.



## References

- [1] Feynman, R. 1983. *Tiny Computers Obeying Quantum Mechanical Laws*. Talk delivered at Los Alamos National Laboratory. Published in *New Directions in Physics: The Los Alamos 40th Anniversary Volume*.
- [2] Peter W. Shor *Polynomial-Time Algorithms for Prime Factorization and Discrete Logarithms on a Quantum Computer*, 1995; arXiv:quant-ph/9508027v2
- [3] Peter W. Shor "Scheme for reducing decoherence in quantum computer memory", 1995; <https://doi.org/10.1103/PhysRevA.52.R2493>
- [4] Daniel Gottesman "An Introduction to Quantum Error Correction and Fault-Tolerant Quantum Computation", 2009; arXiv:0904.2557 [quant-ph]
- [5] Daniel Gottesman "Fault-Tolerant Quantum Computation with Higher-Dimensional Systems", 1998; arXiv:quant-ph/9802007
- [6] A.Yu. Kitaev, "Fault-tolerant quantum computation by anyons", 1997; arXiv:quant-ph/9707021
- [7] John B. Kogut "An introduction to lattice gauge theory and spin systems" 1979; <https://doi.org/10.1103/RevModPhys.51.659>
- [8] Eric Dennis, Alexei Kitaev, Andrew Landahl and John Preskill "Topological quantum memory", 2001; arXiv:quant-ph/0110143
- [9] D. S. Wang, A. G. Fowler, A. M. Stephens, L. C. L. Hollenberg "Threshold Error Rates for the Toric and Surface Codes", 2009; arXiv:0905.0531v1
- [10] Barbara M. Terhal, "Quantum Error Correction for Quantum Memories", 2015; arXiv:1302.3428v7
- [11] Stephen S. Bullock, Gavin K. Brennen "Qudit surface codes and gauge theory with finite cyclic groups" 2006; arXiv:quant-ph/0609070
- [12] O. Viyuela, A. Rivas and M. A. Martin-Delgado "Generalized toric codes coupled to thermal baths", 2012; arXiv:1112.1017
- [13] Razieh Mohseninia, Saeed S. Jahromi, Laleh Memarzadeh and Vahid Karimipour "Quantum phase transition in the Z3 Kitaev-Potts model" 2015; arXiv:1503.05957

- [14] Courtney G. Brell "A proposal for self-correcting stabilizer quantum memories in 3 dimensions(or slightly less)", 2016; arXiv:1411.7046
- [15] Sergey Bravyi, Matthew B Hastings, and Spyridon Michalakis "Topological quantum order: Stability under local perturbations" , 2010; <https://doi.org/10.1063/1.3490195>
- [16] John Dengis, Robert König, and Fernando Pastawski "An optimal dissipative encoder for the toric code" 2014; arXiv:1310.1036
- [17] Justyna Łodyga, Paweł Mazurek, Michal Horodecki "Simple scheme for encoding and decoding a qubit in unknown state for various topological codes" 2015; DOI: 10.1038/srep0897
- [18] Sergey Bravyi and Barbara M. Terhal "A no-go theorem for a two-dimensional self-correcting quantum memory based on stabilizer codes" 2008; arXiv:0810.1983v2
- [19] R. Alicki, M. Fannes and M. Horodecki "On thermalization in Kitaev's 2D model", 2008; arXiv:0810.4584v1
- [20] Anna Komar, Olivier Landon-Cardinal, and Kristan Temme "Self correction requires Energy Barrier for Abelian quantum doubles", 2016; arXiv:1601.01324
- [21] Robert Alicki, Michal Horodecki, Pawel Horodecki, and Ryszard Horodecki "On thermal stability of topological qubit in Kitaev's 4d model", 2008; arXiv:0811.0033
- [22] Sam Roberts and Stephen D. Bartlett "Symmetry-protected self-correcting quantum memories" 2020; arXiv:1805.01474v3
- [23] Adrian Hutter, James R. Wootton, Beat Rothlisberger, and Daniel Loss "Self-correcting quantum memory with a boundary" 2012; arXiv:1206.0991v3
- [24] R. de-Picciotto, M. Reznikov, M. Heiblum, V. Umansky, G. Bunin and D. Mahalu "Direct Observation of a Fractional Charge" 1997; arXiv:cond-mat/9707289
- [25] Liang Jiang, Gavin K. Brennen, Alexey V. Gorshkov, Klemens Hammerer, Mohammad Hafezi, Eugene Demler, Mikhail D. Lukin, and Peter Zoller "Anyonic interferometry and protected memories in atomic spin lattices", 2007; arXiv:0711.1365v1

- [26] J. K. Pachos, W. Wieczorek, C. Schmid, N. Kiesel, R.Pohlner, and H. Weinfurter *Revealing anyonic features in a toric code quantum simulation* 2009; arXiv:0710.0895v3
- [27] Sankar Das Sarma<sup>1</sup>, Michael Freedman, Chetan Nayak *"Topologically-Protected Qubits from a Possible Non-Abelian Fractional Quantum Hall State"*, 2004; arXiv:cond-mat/0412343v2
- [28] Sergey Bravyi and Alexei Kitaev *"Universal quantum computation with ideal Clifford gates and noisy ancillas"*, 2004; arXiv:quant-ph/0403025v2
- [29] James R. Wootton, Jiannis K. Pachos *"Universal Quantum Computation with Abelian Anyon Models"* 2009; arXiv:0904.4373v2
- [30] Benjamin J. Brown, Abbas Al-Shimary, and Jiannis K. Pachos *"Entropic Barriers for Two-Dimensional Quantum Memories"*, 2013; arXiv:1307.6222v3
- [31] Jiannis K. Pachos *"Introduction to topological quantum computation"*, 2012; Cambridge University Press
- [32] Juan Pablo Ibieta Jimenez, *"Topological Order and the Kitaev Model (Seminar)"*, 2016; DOI: 10.13140/RG.2.2.36305.53605
- [33] John Preskill, *online notes from Caltech lectures*
- [34] Anna Kómar *"Quantum Computation and Information Storage in Quantum Double Models"* 2018; phd thesis
- [35] Michael A. Nielsen and Isaac L. Chuang *Quantum Computation and Quantum Information* 2000; Cambridge University Press